BEST AVAILABLE IMAGES

Defective images within this document are accurate representations of the original documents submitted by the applicant.

Defects in the images may include (but are not limited to):

- BLACK BORDERS
- TEXT CUT OFF AT TOP, BOTTOM OR SIDES
- FADED TEXT
- ILLEGIBLE TEXT
- SKEWED/SLANTED IMAGES
- COLORED PHOTOS
- BLACK OR VERY BLACK AND WHITE DARK PHOTOS
- GRAY SCALE DOCUMENTS

IMAGES ARE BEST AVAILABLE COPY.

As rescanning documents *will not* correct images, please do not report the images to the Image Problem Mailbox.

PATENT
ATTORNEY DOCKET NO. 07891/009004

Certificate of Mailing: Date of Deposit: June 14, 2004

I hereby certify under 37 C.F.R. § 1.8(a) that this correspondence is being deposited with the United States Postal Service as first class mail with sufficient postage on the date indicated above and is addressed to Commissioner for Patents, P.O. Box 1450, Alexandria, VA 22313-1450.

Caryn Scafati
Printed name of person mailing correspondence

Caryn Scafati
Signature of person mailing correspondence

IN THE UNITED STATES PATENT AND TRADEMARK OFFICE

Applicant:	Robert G. Korneluk et al.	Art Unit:	1635
Serial No.:	09/974,592	Examiner:	Janet L. Epps
Filed:	October 9, 2001	Customer No.:	21559
Title:	DETECTION AND MODULATION OF IAPS AND NAIP FOR THE DIAGNOSIS AND TREATMENT OF PROLIFERATIVE DISEASE		

Commissioner for Patents
P.O. Box 1450
Alexandria, VA 22313-1450

DECLARATION OF DR. ERIC LACASSE UNDER 37 C.F.R. § 1.132 TRAVERSING GROUNDS OF REJECTION

Under 37 C.F.R.§ 1.132, I declare:

1. I am Senior Scientist and Head of the Department of Oncology at Aegera Therapeutics, Inc, and have published 16 papers relating to IAPs, cancer biology, and antisense therapeutics.

2. I have read the Office Action mailed on August 8, 2003.

3. As disclosed in our specification, antisense oligonucleotides are designed using computer algorithms and screened *in vitro* to identify those that

effectively inhibit protein expression (pages 54-55). Antisense oligonucleotides that are selected for efficacy *in vitro* are typically effective *in vivo*, as well. *In vivo* screening is used to identify those antisense oligonucleotides having the greatest efficacy (pages 55 and 56). Such screening is merely routine.

4. Antisense oligonucleotides are potent and specific therapeutic molecules that share a common mechanism of action: they interfere with protein production by binding to a complementary target mRNA. This binding inhibits protein production by interfering with the ribosome's ability to translate the mRNA, by interfering with splicing, and/or by inducing the degradation of the mRNA by RNAse H, an enzyme that recognizes and degrades mRNA/DNA hybrids. Regardless of the length of the antisense oligonucleotide, if it binds an accessible site on the target RNA in the cell, the antisense oligonucleotide will successfully inhibit protein production.

5. The results shown in Exhibits A (Shankar et al., J. of Neurochem. 79:426-436, 2001, hereafter "Shankar"), B (Kallio et al. FASEB J. express article, 10.1096/fj.01-0280fj3, 2001, hereafter "Kallio"), and C (Fukuda et al. Blood 100:2463-2471, 2002, hereafter "Fukuda"), previously of record, were carried out using methods available at the time applicants' priority document was filed. These references describe the use of antisense oligonucleotides of varying lengths to decrease the expression of an inhibitor of apoptosis protein, i.e., human survivin.

6. Shankar describes the use of phosphorothioate modified antisense oligonucleotides, 20 nucleotides in length, to downregulate expression of human survivin expression and to induce apoptosis in neural tumor cells in culture.

7. Kallio describes the use of phosphorothioate modified antisense oligonucleotides, 18 nucleotides in length, to downregulate human survivin expression in HeLa and PtK1 cells in culture. The antisense oligonucleotides were conjugated to fluorescein isothiocyanate, which allowed them to be visualized by fluorescence microscopy.

8. Fukuda describes the use of a full-length antisense survivin expression construct to modulate survivin expression in CD34 cells.

9. In further support of the enablement of the claimed methods, provided herewith are U.S. Patent Nos. 5,958,771 ("the '771 patent") and 5,958,772 ("the '772 patent"), which were filed on December 3, 1998, and 6,087,173 ("the '173 patent"), which was filed on September 9, 1999, (Exhibits E, F, and G, respectively). As detailed below, each of these patents relates to the use of phosphorothioate modified antisense oligonucleotides to inhibit the expression of an IAP, and each of the cited examples was carried out using methods available at the time applicants' priority document was filed.

10. The '771 patent describes the identification of twelve phosphorothioate modified 18-mer oligodeoxynucleotides that inhibited Cellular Inhibitor of Apoptosis-2 (cIAP-2) expression in cells *in vitro* (Table 1 and column 41, first paragraph).

11. The '772 patent describes the identification of six 18-mer phosphorothioate oligodeoxynucleotides that inhibited cIAP-1 expression in cells *in vitro* (Table 1 and column 39, first paragraph).

12. The '173 patent describes the identification of twenty-four phosphorothioate modified 20-mer antisense oligodeoxynucleotides that inhibited XIAP expression in cells in vitro (Table 1, and column 41, first paragraph).

13. The examples cited below, and reviewed by Jansen, Exhibit D, which relate to the use of phosphorothioate modified antisense oligonucleotides to inhibit protein production, were also carried out using methods available at the time applicants' priority document was filed.

14. Jansen describes phase I trials, which were carried out in 1997, using an 18-mer phosphorothioate Bcl-2 antisense oligonucleotide (page 676, right column, first paragraph) to treat non-Hodgkin lymphoma. The 18-mer antisense oligonucleotide decreased BCL-2 protein levels in half of all patients that received it.

15. In a 1996 study by Yazaki et al. (Mol Pharmacol 50:236-42, 1996), which is also reviewed by Jansen, a 20-mer phosphorothioate Protein Kinase C antisense oligonucleotide was used to inhibit glioblastoma xenografts in mice (paragraph spanning page 677, right column, to page 678, left column).

16. A clinical pilot study, carried out by Ratjczak and colleagues in 1992 is also reviewed in Jensen. In this study, a 24-mer phosphorothioate antisense oligonucleotide was used *ex vivo* to target the c-MYB proto-oncogene in bone-

marrow cells harvested from patients with chronic myelogenous leukemia (page 679, right column, first paragraph).

17. As further evidence of enablement, provided herewith are Exhibits H (Sugano et al., J. Biol. Chem. 271:19080-19083, 1996, hereafter "Sugano"), I (Galvin-Parton et al., J. Biol. Chem. 272: 4335-4341, 1997, hereafter "Galvin-Parton"), J (MacLeod et al., J. Biol. Chem. 270:8037-8043, 1995, hereafter "MacLeod"), and K (Ramchandani et al., P.N.A.S. 94:684-689, 1997, "Ramchandani"), all of which were received for publication prior to the date on which applicants' priority document was filed, and all of which relate to methods of using antisense oligonucleotides to inhibit protein production.

18. Sugano, published in 1996, used a 21-mer antisense oligonucleotide to inhibit expression of cholesteryl ester transfer protein (CETP), the enzyme that facilitates the transfer of cholesterylester from high density lipoprotein to apoB-containing lipoprotein. The asialoglycoprotein-coupled 21-mer antisense oligonucleotide, which was administered to rabbits intravenously, decreased CETP biological activity and also decreased total cholesterol levels.

19. As published in February 1997, Galvin-Parton expressed a 39-mer antisense oligonucleotide in transgenic mice. This 39-mer antisense oligonucleotide, which targeted the nucleic acid encoding G-protein, $G\alpha_q$, decreased $G\alpha_q$ polypeptide levels, and caused an increase in body mass and hyperadiposity.

20. MacLeod, in 1995, expressed a 600-mer antisense oligonucleotide, which was complementary to DNA methyltransferase mRNA, in Y1 cells, a tumorigenic adrenocortical cell line. This antisense oligonucleotide decreased DNA methyltransferase gene expression, protein activity, and also decreased the ability of the Y1 cells to form tumors when injected into mice.

21. In a related study published in January 1997, Ramchandani designed a phosphorothioate modified 20-mer antisense oligonucleotide that targeted the same region of DNA methyltransferase mRNA that was targeted by the 600-mer described by MacLeod. Ramchandani injected tumorigenic Y1 cells into the flanks of mice, allowed tumors to form, then administered the 20-mer antisense oligonucleotide to the tumor. The 20-mer and the 600-mer antisense oligonucleotides, though of widely differingly lengths, both decreased DNA methyltransferase levels and inhibited tumor growth.

22. In sum, Shankar, Kallio, Fukuda, the '771 patent, the '772 patent, the '173 patent, Jansen, Sugano, Galvin-Parton, and MacLeod describe the use of antisense oligonucleotides that range in length between 18 and 600 nucleotides to inhibit the expression of a target gene and achieve a desired biological effect. These antisense oligonucleotides, regardless of length, bind to a complementary target mRNA and inhibit protein production, just as applicants' antisense oligonucleotides do. One skilled in the field of antisense, being familiar with the art available at the time of filing (of which the above is but a sample) would know

that antisense molecules complementary to a portion of XIAP could be a variety of different lengths.

23. I hereby declare that all statements made herein of my own knowledge are true and that all statements made on information and belief are believed to be true; and further that these statements were made with the knowledge that willful false statements and the like so made are punishable by fine or imprisonment, or both, under Section 1001 of Title 18 of the United States Code and that such willful false statements may jeopardize the validity of the application or any patents issued thereon.

Date: June 11, 2004

Dr. Eric Lacasse

EXHIBIT H

THE JOURNAL OF BIOLOGICAL CHEMISTRY
Vol. 271, No. 32, Issue of August 9, pp. 19080–19083, 1996
Printed in U.S.A.

Changes in Plasma Lipoprotein Cholesterol Levels by Antisense Oligodeoxynucleotides against Cholesteryl Ester Transfer Protein in Cholesterol-fed Rabbits*

(Received for publication, March 14, 1996, and in revised form, May 14, 1996)

Masahiro Sugano‡ and Naoki Makino

From the Department of Bioclimatology and Medicine, Medical Institute of Bioregulation, Kyushu University, 4546 Tsurumihara, Beppu, Oita 874, Japan

Cholesteryl ester transfer protein (CETP) is the enzyme that facilitates the transfer of cholesteryl ester from high density lipoprotein (HDL) to apoB-containing lipoproteins and also affects the low density lipoprotein metabolism. On the other hand, the liver is the major tissue responsible for the production of CETP (CETP mRNA) in rabbits. To test the hypothesis that a reduction of CETP mRNA in the liver by antisense oligodeoxynucleotides (ODNs) may affect the plasma lipoprotein cholesterol levels, we intravenously injected antisense ODNs against rabbit CETP coupled with asialoglycoprotein carrier molecules, which serve as an important method to regulate liver gene expression, to cholesterol-fed rabbits via their ear veins. All rabbits were fed a standard rabbit chow supplement with 0.1% cholesterol for 10 weeks before and throughout the experiment. After injecting rabbits with antisense ODNs, the plasma total cholesterol concentrations and plasma CETP activities all decreased at 24, 48, and 96 h, whereas the plasma HDL cholesterol concentrations increased at 48 h. A reduction in the hepatic CETP mRNA was also observed at 6, 24, and 48 h after the injection with antisense ODNs. However, in the rabbits injected with sense ODNs, the plasma total and HDL cholesterol concentrations and the plasma CETP activities did not significantly change, and the hepatic CETP mRNA did not change either throughout the experimental period. Although the exact role of CETP in the development of atherosclerosis remains to be clarified, these findings showed for the first time that the intravenous injection with antisense ODNs against CETP coupled to asialoglycoprotein carrier molecules targeted to the liver could thus inhibit plasma CETP activity and, as a result, could induce a decrease in the plasma low density lipoprotein and very low density lipoprotein cholesterol and an increase in the plasma HDL cholesterol in cholesterol-fed rabbits.

Cholesteryl ester transfer protein (CETP)[1] is a plasma glycoprotein that catalyzes the transfer of cholesteryl ester and triglyceride among lipoproteins (1, 2). CETP deficiency in humans (3–5) has been proposed to be associated with longevity (3). The homozygotes for CETP deficiency demonstrated markedly elevated HDL-C and plasma apoA-I levels as well as decreased LDL cholesterol and plasma apoB levels (4, 6). CETP-deficient subjects have also been found to have a substantially increased catabolic rate of apoB as the primary metabolic basis for the low plasma levels of LDL apo B (7). This finding indicates that the LDL receptor pathway may thus be up-regulated during CETP deficiency. It has also been proposed that a CETP deficiency may be associated with protection against ischemic heart disease, based on the observed longevity in one kindred (3), as well as the lack of any evidence of coronary heart disease (6) in other kindreds with CETP deficiency; however, these findings remain controversial. Several other lines of evidence also support the hypothesis. The plasma level of CETP is directly correlated with the extent of coronary atherosclerosis in monkeys fed a cholesterol diet (8). A transgenic mouse overexpressing simian CETP developed accelerated atherosclerosis (9). Thus, the inhibition of plasma CETP activity may potentially be a novel method of reducing the plasma levels of LDL cholesterol by enhancing LDL catabolism (7) and decreasing the transfer of cholesteryl ester from HDL to apoB-containing lipoproteins (1, 2). Since the liver is the major tissue responsible for the production of CETP (CETP mRNA) in rabbits (10, 11) (even though adipose tissue may also be the major tissue responsible for the production of CETP in monkeys (12)), a reduction of CETP in the liver by antisense oligodeoxynucleotides (ODNs) may thus cause a reduction in the plasma LDL and/or VLDL cholesterol concentrations. The present study was therefore undertaken to determine the effect of an intravenous injection with antisense ODNs to the liver on the CETP mRNA expression, plasma CETP activity and plasma cholesterol concentrations in rabbits fed a low cholesterol diet. These antisense ODNs were originally designed to be coupled with asialoglycoprotein carrier molecules, and this coupling serves as an important method to regulate liver gene expression (13).

MATERIALS AND METHODS

Construction of ODNs—The sequences of ODNs against rabbit CETP used in this study were as follows: antisense, 5′-CTTGACCCGGCCGAGGAGCAT-3′; sense, 5′-ATGCTCCTCGGCCGGGTCAAG-3′, positions +148 to +168 of the rabbit sequence (11). These selected target sequences have relatively low homology with any of the other known cDNA sequences found in the GenBank data base. The synthetic ODNs were purified on the column, dried down, resuspended in Tris-EDTA (10 mM Tris, pH 7.4, and 1 mM EDTA), and then quantitated by spectrophotometry. Asialoglycoprotein-poly-L-lysine (M_r approximately 71,400), which was prepared according to the method of Wu and Wu (14) and Wu *et al.* (15), was added to the ODNs (at a molar ratio of 25:1) with vigorous mixing. The solution was incubated at 4 °C overnight and dialyzed (two times) against 0.15 M saline (1500:1; membrane M_r cutoff, 3500). The samples were electrophoresed through a 2% agarose gel using Tris/borate/EDTA buffer and then stained with ethidium bromide to visualize DNA. The samples were filtered through a 0.2-μm mem-

* The costs of publication of this article were defrayed in part by the payment of page charges. This article must therefore be hereby marked "*advertisement*" in accordance with 18 U.S.C. Section 1734 solely to indicate this fact.

‡ To whom correspondence should be addressed. Tel.: 81-977-24-5301; Fax: 81-977-24-8945.

[1] The abbreviations used are: CETP, cholesteryl ester transfer protein; HDL, high density lipoprotein; LDL, low density lipoprotein; ODN, oligodeoxynucleotide; VLDL, very low density lipoprotein; PCR, polymerase chain reaction.

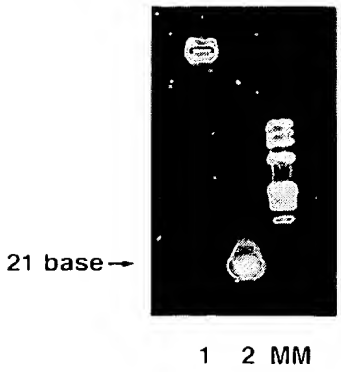

FIG. 1. **Asialoglycoprotein-poly-L-lysine-ODN complex and ODNs alone were electophoresed through 2% agarose gel using a Tris/borate/EDTA buffer and then were stained with ethidium bromide to visualize DNA.** *Lane 1,* asialoglycoprotein-poly-L-lysine-ODN-complex; *lane 2,* ODNs alone; *MM, Hae*III molecular marker.

brane (Millipore Corp., Bedford, MA) before injection.

Experimental Protocol—Twenty-six male Japanese white rabbits weighing 2.0–2.5 kg were used in the experiment. All animals were housed individually, had free access to water, and were fed a standard rabbit chow supplement with 0.1% cholesterol for 10 weeks before and throughout the experiment. The plasma total and HDL cholesterol concentrations, which did not significantly change between the period after 9 and 10 weeks of feeding, were determined. Thirteen animals were injected with asialoglycoprotein-poly-L-lysine-antisense ODN complex, whereas the remaining 13 animals were injected with asialoglycoprotein-poly-L-lysine-sense ODN complex via the ear veins. The amount of ODNs injected was 30 μg/kg for each rabbit. At 6, 24, 48, and 96 h after injection, two rabbits in each group were killed, and liver specimens were taken. At the same time, about 1 ml of the blood was drawn from the remaining animals via their ear veins.

Measurement of CETP mRNA—Total RNA was isolated from the liver with a RNAzolB solution (Biotex, Friendswood, TX) according to the the manufacturer's procedure with slight modifications (12). The abundance of CETP mRNA was determined by quantitative dot blotting (16). The rabbit cRNA probe labeled with fluorescein-dUTP was produced by the nonradiolabeled, reverse transcription polymerase chain reaction (PCR) (Amersham Corp.), according to the rabbit sequence (11). The sense and antisense primers used for PCR, the sizes of the PCR products, and the PCR cycles in each cRNA probe were: CETP, sense, 5'-CTTTCCATAAACTGCTCCTG-3'; antisense, 5'-CCTGGGTCTCCGCACTTTCT-3'; size, 482 base pairs; 30 cycles; and glyceraldehyde-3-phosphate dehydrogenase, sense, 5'-ATGGTCTACATGTTCCAGTA-3'; antisense, 5'-TAAGCAGTTGGTGGTGCAGG-3'; size, 343 base pairs; 30 cycles.

Biochemical Analysis—The plasma cholesterol concentrations were measured in whole plasma and in the HDL-containing supernatant after the precipitation of VLDL and LDL with dextran-Mg^{2+} using the Wako total and HDL cholesterol measuring kit (Wako Ltd., Osaka, Japan). The plasma constituents related to liver function were analyzed using an automatic analyzer (Hitachi Ltd., Tokyo, Japan). The CETP activity in the plasma was determined by a radioassay according to the modified method of Yen *et al.* (17). A volume of 20 μl of plasma was incubated for 30 min at 37 °C in the presence of [^{3}H]cholesteryl oleate-labeled HDL (3–10 nmol CE) and an excessive amount of VLDL and LDL (0.2 μmol of CE). The volume was adjusted to 200 μl with Tris-saline (pH 7.4) before incubation. After the precipitation of VLDL and LDL by heparin and $MnCl_2$ (18), half of the supernatant volume was then removed and counted in a liquid scintillation counter.

Statistical Analysis—All values are presented as the mean ± standard error of the mean. The statistical analysis was performed by a paired *t* test for comparisons in the intragroup and by Student's *t* test for comparisons between the groups. Differences were considered statistically significant at a value of $p < 0.05$.

RESULTS

We characterized the asialoglycoprotein-ODN complex by gel electrophoresis. The samples were electrophoresed through a 2% agarose gel using Tris/borate/EDTA buffer and then were stained with ethidium bromide to visualize DNA (Fig. 1). The

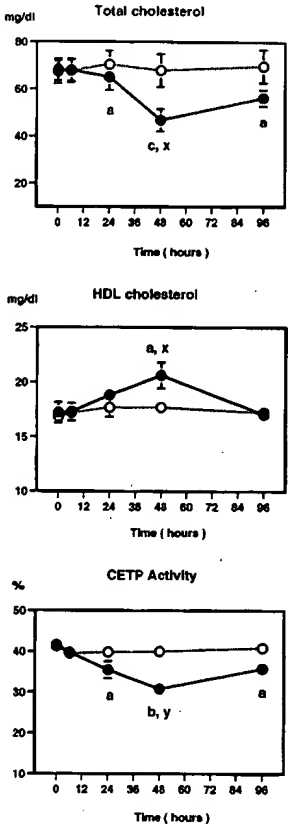

FIG. 2. **Changes in the plasma cholesterol concentrations and plasma CETP activities.** Concentrations were measured at 0 (n = 13), 6 (n = 11), 24 (n = 9), 48 (n = 7), and 96 (n = 5) h for each group. ●, rabbits injected with antisense ODNs; O, rabbits injected with sense ODNs. Values are mean ± S.E. *a*, $p < 0.05$; *b*, $p < 0.01$; *c*, $p < 0.001$ compared with 0 h, as determined by a paired *t* test. *X*, $p < 0.05$; *y*, $p < 0.01$ compared with rabbits injected with sense ODNs, as determined by Student's *t* test.

ODNs were retained by the asialoglycoprotein-poly-L-lysine conjugate in the well, whereas ODNs alone entered the gel. In the rabbits injected with antisense ODNs, the total cholesterol concentrations and the CETP activities were all significantly decreased at 24, 48, and 96 h compared with those at 0 h. At 48 h, the total cholesterol concentrations and the CETP activities were also significantly lower in the rabbits injected with antisense ODNs than in those injected with sense ODNs (Fig. 2). The HDL cholesterol concentrations significantly increased at 48 h compared with those at 0 h and the rabbits injected with sense ODNs (Fig. 2). In the rabbits injected with sense ODNs, the total and HDL cholesterol concentrations and the CETP activities did not significantly change throughout the experiment (Fig. 2). Fig. 3 shows a typical example of the dot blot analyses of hepatic CETP mRNA treated with antisense ODNs. A reduction of hepatic CETP mRNA was observed at 6, 24, and 48 h after injection with antisense ODNs. When the amount of hepatic CETP mRNA was measured by scanning and expressed as a ratio to glyceraldehyde-3-phosphate dehydrogenase mRNA, the mean values were 0.83 (100%) at 0 h, 0.43 (51.8%) at 6 h, 0.40 (48.2%) at 24 h, 0.65 (78.3%) at 48 h, and 0.87 (104.8%) at 96 h (the parentheses express the percentages against the value at 0 h). Hepatic CETP mRNA treated with sense ODNs did not change throughout the experimental period (data not shown). We measured the plasma constituents related to liver function (aspartate aminotransferase, alanine aminotransferase γ-GTP, alkaline phosphatase, and total bilirubin), including triglyceride in the rabbits (data not shown). These levels did not significantly change throughout the exper-

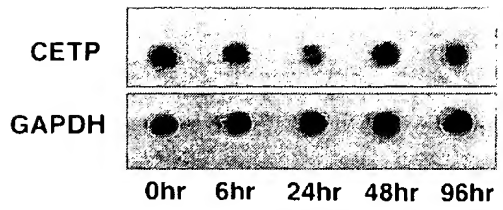

FIG. 3. **Dot blot analyses of hepatic CETP mRNA treated with antisense ODNs.** Glyceraldehyde-3-phosphate dehydrogenase mRNA (*GAPDH*) is indicated as the control.

imental period and were also not significantly different between the animals injected with sense and antisense ODNs.

DISCUSSION

In the present study, an injection of asialoglycoprotein-poly-L-lysine-antisense complex reduced the hepatic CETP mRNA, plasma CETP activities, and plasma total cholesterol, whereas it increased HDL cholesterol concentrations. The antisense ODNs used in the present study demonstrated no side effects within 4 days after injection. The antisense ODNs are widely used as inhibitors of specific gene expression because they offer the possibility of blocking the expression of a particular gene without any changes in the functions of other genes (19). However, for successful antisense delivery, some criteria must be fulfilled (19–21). Recently, an efficient gene transfer method mediated by a viral liposome complex has been used as a delivery system of antisense ODNs *in vivo* (22–24). However, to use the methods mentioned above, many technical and methodological difficulties still need to be overcome in comparison with those in our study, and such gene targeting is also troublesome to use in chronic clinical situations, such as in the treatment of atherosclerosis. Regarding lipoprotein metabolism, almost all enzymes and apolipoproteins are produced in the liver; therefore, the efficient receptor-mediated delivery of antisense ODNs to the liver *in vivo* used in our study may be useful for both diagnostic and therapeutic applications for lipoprotein metabolism. In our study, the total cholesterol concentrations and the CETP activities were all significantly decreased at 24, 48, and 96 h, whereas the HDL cholesterol concentrations significantly increased only at 48 h compared with those at 0 h. At 48 h, the total cholesterol decreased substantially more than the HDL cholesterol increased (Fig. 2). Although we could not conclusively clarify the exact reason for these results, the following factors are considered to play a role. The assay used for the CETP activity in this study cannot always show the true CE mass transfer *in vivo*, because the assay uses exogenous lipoprotein substrates added in the assay, whereas *in vivo* the CE is transferred among the endogenous lipoproteins of plasma (25). This may partly explain why the CETP activity is still significantly reduced at 96 h, whereas the HDL cholesterol levels returned to normal. It has been reported that there is an inverse relationship between the plasma CETP and liver LDL receptor mRNA in CETP transgenic mice (26). The induced LDL receptor expression in LDL receptor transgenic mice leads to a marked reduction in plasma VLDL and LDL (27), possibly because approximately 50–80% of VLDL and/or LDL is cleared by hepatocytes, due to LDL receptor-mediated endocytosis (28, 29). LDL receptor protein and activity are generally parallel to LDL receptor mRNA levels (27). It is also indicated that the reduction of plasma CETP reduces the plasma levels of LDL and VLDL cholesterol possibly by enhancing LDL catabolism (7) and possibly by decreasing the transfer of cholesteryl ester from HDL to apoB-containing lipoproteins (1, 2), and it also increases the plasma level of HDL cholesterol, possibly due to the latter reason. Since normal rabbits have a large degree of CETP activity (30), and the LDL receptor is down-regulated, and CETP mRNA in the liver and plasma CETP increase especially in the rabbits fed an atherogenic diet more than in those fed a standard diet (10), the inhibition of CETP by antisense ODNs in our study may thus affect not only the decrease in CETP but also the increase in the LDL receptor much more than other models. Thus, as a result, the VLDL and LDL cholesterol levels might be reduced more than the HDL level was increased. Our antisense injection was considered successful for the following reasons: (*a*) the asialoglycoprotein-poly-L-lysine-antisense complex is rapidly and preferentially taken up by the liver (13) and has enhanced resistance to nuclease degradation in plasma (31); (*b*) the amount of CETP mRNA in the liver is thought to be relatively low compared with other lipoprotein mRNAs in the liver; however, these findings have only been previously seen in the cynomolgus monkey (12); and (*c*) the liver is the major tissue responsible for the production of CETP (CETP mRNA) in rabbits (10, 11) (although adipose tissue may also be found in monkeys (12)). The exact role of CETP in the development of atherosclerosis has yet to be clarified. Marotti *et al.* (9) demonstrated that transgenic mice expressing cynomolgus monkey CETP had significantly more early atherosclerotic lesions in the proximal aorta than controls when fed a high cholesterol diet. On the other hand, more recently Hayek *et al.* (32) concluded that CETP expression inhibited the development of early atherosclerotic lesions in hypertriglyceridemic mice. The CETP expression in hypertriglyceridemic animals produced a much greater reduction in the HDL size (33). These small particles, which can be produced by CETP (34), may thus be an optimal mediator of cellular cholesterol efflux (35).

In conclusion, in this study we have shown that the intravenous administration of the asialoglycoprotein-poly-L-lysine-antisense complex is a beneficial method for reducing the plasma levels of LDL and VLDL cholesterol and increasing the plasma level of HDL cholesterol, possibly by enhancing LDL catabolism (7) and decreasing the transfer of cholesteryl ester from HDL to apoB-containing lipoproteins (1, 2). However, it must be mentioned that our results were limited to the period comprising only several days after the injection. Therefore, to elucidate the exact effect of CETP on atherosclerosis development, further longer term studies are called for.

Acknowledgments—We thank Sachiyo Taguchi and Miha Watanabe for their expert technical assistance.

REFERENCES

1. Tall, A. R. (1986) *J. Lipid Res.* **27,** 361–367
2. Hesler, C. B., Swenson, T. L., and Tall, A. R. (1987) *J. Biol. Chem.* **262,** 2275–2282
3. Saito, F. (1984) *Metab. Clin. Exp.* **33,** 629–633
4. Koizumi, J., Mabuchi, H., Yoshimura, A., Michishita, I., Takeda, M., Itoh, H., Sakai, Y., Sakai, T., Ueda, K., and Takeda R. (1985) *Atherosclerosis* **58,** 175–186
5. Brown, M. L., Inazu, A., Hesler, C. B., Agellon, L. B., Mann, C., Whitlock, M. E., Marcel, Y. L., Milne, R. W., Koizumi, J., Mabuchi, H., and Tall, A. R. (1989) *Nature* **342,** 448–451
6. Inazu, A., Brown, M. L., Hesler, C. B., Agellon, L. B., Koizumi, J., Tanaka, K., Maruhama, Y., Mabuchi, H., and Tall, A. R. (1990) *N. Engl. J. Med.* **323,** 1234–1238
7. Ikewaki, K., Nishiwaki, M., Sakamoto, T., Ishikawa, T., Fairwell, T., Zech, L. A., Nagano, M., Nakamura, H., Brewer, H. B., Jr., and Rader, D. J. (1995) *J. Clin. Invest.* **96,** 1573–1581
8. Quinet, E., Tall, A. R., Ramakrishnan, R., and Rudel, L. (1992) *J. Clin. Invest.* **87,** 1559–1566
9. Marotti, K. R., Castle, C. K., Boyle, T. P., Lin, A. H., Murray, R. W., and Melchior, G. W. (1993) *Nature* **364,** 73–75
10. Quinet, E. M., Agellon, L. B., Kroon, P. A., Marcel, Y. L., Lee, Y. C., Whitlock, M. E., and Tall, A. R. (1990) *J. Clin. Invest.* **85,** 357–363
11. Nagashima, M., McLean, J. W., and Lawn, R. M. (1988) *J. Lipid Res.* **29,** 1643–1649
12. Pape, M. E., Rehberg, E. F., Marotti, K. R., and Melchior, G. W. (1992) *Arterioscler. Thromb.* **11,** 1759–1771
13. Lu, X. M., Fischman, A. J., Jyawook, S. L., Hendricks, K., Tompkins, R. G., and Yarmush, M. L. (1994) *J. Nucl. Med.* **35,** 269–275
14. Wu, G. Y., and Wu, C. H. (1987) *J. Biol. Chem.* **262,** 4429–4432
15. Wu, G. Y., Wilson, J. M., Shalaby, F., Grossman, M., Shafritz, D. A., and Wu,

C. H. (1991) *J. Biol. Chem.* **266**, 14338–14342
16. Lin-Lee, Y. C., Kao, F. T., Cheung, P., and Chan, L. (1985) *Biochemistry* **24**, 3751–3756
17. Yen, F. T., Deckelbaum, R. J., Mann, C. J., Marcel, Y. L., Milne, R. W., and Tall, A. R. (1989) *J. Clin. Invest.* **83**, 2018–2024
18. Warnick, G. R., and Albers, J. J. (1978) *J. Lipid Res.* **19**, 65–76
19. Helene, C., and Toulme, J. J. (1990) *Biochim. Biophys. Acta* **1049**, 99–125
20. Stein, C. A., and Cheng, Y.-C. (1993) *Science* **261**, 1004–1012
21. Piwnica-Worms, D. (1994) *J. Nucl. Med.* **35**, 1064–1066
22. Morishita, R., Gibbons, G. H., Ellison, K. E., Nakajima, M., Zang, L., Kaneda, Y., Ogihara, T., and Dzau, V. J. (1993) *Proc. Natl. Acad. Sci. U. S. A.* **90**, 8474–8478
23. Morishita, R., Gibbons, G. H., Ellison, K. E., Nakajima, M., Leyen, H. V. L., Zang, L., Kaneda, Y., Ogihara, T., and Dzau, V. J. (1994) *J. Clin. Invest.* **93**, 1458–1464
24. Tomita, N., Morishita, N., Higaki, J., Aoki, M., Nakamura, Y., Mikami, H., Fukamizu, A., Murakami, K., Kaneda, Y., and Ogihara, T. (1995) *Hypertension* **26**, 131–136
25. Mann, C. J., Yen, F. T., Grant, A. M., and Bihain, B. E. (1991) *J. Clin. Invest.* **88**, 2059–2066
26. Jiang, X. C., Masucci-Magoulas, L., Mar, J., Lin, M., Walsh, A., Breslow, J. L., and Tall, A. (1993) *J. Biol. Chem.* **268**, 27406–27412
27. Yokode, M., Hammer, R. E., Ishibashi, S., Brown, M. S., and Goldstein, J. L. (1990) *Science* **250**, 1273–1275
28. Spady, D. K., Bilheimer, D. W., and Dietschy, J. M. (1983) *Proc. Natl. Acad. Sci. U. S. A.* **80**, 3499–3503
29. Spady, D. K., and Dietschy, J. M. (1985) *J. Lipid Res.* **26**, 465–472
30. Ha, Y. C., and Barter, P. J. (1982) *Comp. Biochem. Physiol.* **71B**, 265–269
31. Chiou, H. C., Tangco, M. V., Levine, S. M., Robertson, D., Kormis, K., Wu, C. H., and Wu, G. Y. (1994) *Nucleic Acids Res.* **22**, 5439–5446
32. Hayek, T., Masucci-Magoulas, L., Jiang, X., Walsh, A., Rubin, E., Breslow, J. L., and Tall, A. R. (1995) *J. Clin. Invest.* **96**, 2071–2074
33. Hayek, T., Chajek-Shaul, T., Walsh, A., Agellon, L. B., Moulin, P., Tall, A. R., and Breslow, J. L. (1992) *J. Clin. Invest.* **90**, 505–510
34. Sugano, M., Shah, R., and Rudel, L. L. (1991) *Circulation* **84**, 378a (abstr.)
35. Fielding, C. J., and Fielding, P. E. (1995) *J. Lipid. Res.* **36**, 211–228

THE JOURNAL OF BIOLOGICAL CHEMISTRY

Vol. 272, No. 7, Issue of February 14, pp. 4335–4341, 1997
Printed in U.S.A.

Induction of $G\alpha_q$-specific Antisense RNA *in Vivo* Causes Increased Body Mass and Hyperadiposity*

(Received for publication, August 26, 1996, and in revised form, November 29, 1996)

Patricia A. Galvin-Parton‡, Xiaohui Chen‡, Christopher M. Moxham§, and Craig C. Malbon§¶

From the Departments of ‡Pediatrics and §Molecular Pharmacology, Diabetes and Metabolic Diseases Research Program, University Medical Center, SUNY/Stony Brook, Stony Brook, New York 11794-8651

Transgenic BDF-1 mice harboring an inducible, tissue-specific transgene for RNA antisense to $G\alpha_q$ provide a model in which to study a loss-of-function mutant of $G\alpha_q$ *in vivo*. $G\alpha_q$ deficiency induced in liver and white adipose tissue at birth produced increased body mass and hyperadiposity within 5 weeks of birth that persisted throughout adult life. $G\alpha_q$-deficient adipocytes display reduced lipolytic responses, shown to reflect a newly discovered, α_1-adrenergic regulation of lipolysis. This α_1-adrenergic response via phosphoinositide hydrolysis and activation of protein kinase C is lacking in the $G\alpha_q$ loss-of-function mutants *in vivo* and provides a basis for the increased fat accumulation.

Heterotrimeric G-proteins (G-proteins)[1] mediate transmembrane signaling from a populous group of cell-surface receptors to a lesser group of effector molecules that includes adenylyl cyclase, phospholipase C, and various ion channels (1). G-proteins have been shown to regulate complex biological processes, including cellular differentiation (2, 3), neonatal development (4–6), and oncogenesis (7). The expression of $G\alpha_o$, for example, is highly localized to the growth cones of developing neurites (2). Suppression of $G\alpha_o$ expression provokes the collapse of developing growth cones (8), whereas expression of constitutively active mutants of $G\alpha_o$ promote increased expression of neurites (9). In adipogenesis of 3T3 L1 embryonic fibroblasts, $G\alpha_s$ acts as a suppressor (2). Inducers of differentiation stimulate a sharp decline in $G\alpha_s$ levels, and constitutive expression of $G\alpha_s$ blocks induction of differentiation (2). $G\alpha_{i2}$ has been shown to regulate the progression of embryonic stem cells to primitive endoderm (4), acting via phospholipase C (PLC) and protein kinase C to suppress progression (10). The morphogen retinoic acid induces primitive endoderm by stimulating a sharp decline in $G\alpha_{i2}$ (4). Mimicking the decline with oligodeoxynucleotides antisense to $G\alpha_{i2}$ provokes progression in the *absence* of retinoic acid (4, 10). Study of G-proteins *in vivo* is a formidable task. The role of $G\alpha_{i2}$ *in vivo* has been studied through inducible, tissue-specific ablation by antisense RNA (5, 6) and gene inactivation by homologous recombination (11). Deficiency in $G\alpha_{i2}$ leads to a runted phenotype (5, 6, 11), insulin resistance (12), and for the transgenic mice with the inactivated $G\alpha_{i2}$ gene, ulcerative colitis and adenocarcinoma of the colon (11).

Little is known about the role of G-proteins of the G_q family *in vivo*. Two highly homologous members of the G_q subfamily of G-proteins, $G\alpha_q$ and $G\alpha_{11}$, can stimulate PLC and are insensitive to pertussis toxin (13–17). $G\alpha_{11}$ have been shown to mediate growth in fibroblasts in response to bradykinin and thrombin (18), hypertrophy in cultured neonatal ventricular myocytes (19), and transformation in NIH 3T3 cells (20). In the current work, we employ conditional, tissue-specific expression of RNA antisense to $G\alpha_q$ in transgenic mice to explore the role of this G-protein *in vivo* and more specifically in white adipocytes made deficient of $G\alpha_q$.

EXPERIMENTAL PROCEDURES

Reagents and Supplies—[^{3}H]cyclic AMP, [^{32}P]dCTP, [γ-^{32}P]ATP, [^{3}H]inositol 1,4,5-trisphosphate (IP_3), Gene Screen Plus, and anti-$G\alpha_{is}$ antibodies (EC2) were purchased from Dupont NEN. All other reagents were purchased from Sigma or standard suppliers (5).

Mice—The B6D2F1 (BDF1) strain of mice was purchased from Taconic Farms Inc. and handled in accordance with the guidelines established by the Institutional Animal Care and Use Committee at the State University of New York at Stony Brook.

Experimental Design of the Antisense RNA Strategy—The pPCK-ASGα_q expression vector was constructed as described below using standard techniques. In order to insert the antisense sequence at the *Bgl*II site within the first exon of the phosphoenolpyruvate carboxykinase (PEPCK) gene, the 7.0-kb PEPCK gene was subcloned as a 1.0-kb *Eco*RI/*Hin*dIII and a 5.8-kb *Hin*dIII/*Bam*HI fragment into the vector pGEM7Zf(+) (Promega). The vector harboring the 1.0-kb gene fragment was digested with *Bgl*II, and the restriction ends were made flush using the Klenow fragment. The 39-bp antisense sequence was obtained within a 235-bp *Nhe*I/*Sst*I fragment excised from the vector pLNC-ASGα_{i2} (4). The restriction ends of this fragment were filled-in, ligated with the *Bgl*II-digested gene fragment, and used to transform XL-1 Blue strain of *Escherichia coli* (Stratagene) under selection with ampicillin. Plasmids with the 1.2-kb fragment and an insert oriented to produce antisense RNA were identified by direct DNA sequencing. The 1.2-kb fragment containing the antisense sequence was digested with *Sac*II and *Cla*I (sites present in the 235-bp sequence harboring the antisense sequence), and a 59-bp oligomer containing the sense sequence to $G\alpha_q$ (−33 to +3) flanked by restriction enzyme sites for *Bcl*I (5′) and *Sal*I (3′) was ligated via force cloning into the *Sac*II and *Cla*I sites. Insertion of the oligomer was confirmed by restriction digest analysis with *Bcl*I and *Sal*I. The presence of unique restriction sites within the 235-bp fragment facilitates the removal and insertion of different antisense sequences in a cassette-like fashion. The 1.2-kb fragment containing the antisense sequence was excised and ligated into the plasmid harboring the 5.8-kb gene fragment to produce the 7.0-kb pPCK-ASGα_q construct. In addition, the synthesis of primers complimentary to the flanking ends of the 235-bp insert allows for discrimination between the pPCK-ASGα_q RNA and the endogenous PEPCK RNA in subsequent reverse transcription-PCR amplification reactions (see below).

In choosing the antisense RNA target sequence, we had to consider

* This work was supported in part by American Cancer Society Award 9400504-DB (to C. C. M.) and a National Institutes of Health, NIDDK Fellowship T32 DK50721 (to C. M. M.). The costs of publication of this article were defrayed in part by the payment of page charges. This article must therefore be hereby marked "*advertisement*" in accordance with 18 U.S.C. Section 1734 solely to indicate this fact.

All authors contributed equally to work reported herein.

¶ To whom all correspondence should be addressed: Dept. of Molecular Pharmacology, DMDRP, University Medical Center, SUNY/Stony Brook, Stony Brook, NY 11794-8651; Tel.: 516-444-7873; Fax: 516-444-7696; E-mail: craig@pharm.som.sunysb.edu.

[1] The abbreviations used are: G-proteins, heterotrimeric G-proteins; PLC, phospholipase C; KRP buffer, Krebs-Ringer phosphate buffer; BSA, bovine serum albumin; PEPCK, phosphoenolpyruvate carboxykinase; IP_3, inositol 1,4,5-trisphosphate; DAG, 1,2-*sn*-diacylglycerol; PCR, polymerase chain reaction; CPT, chlorophenylthio; bp, base pair(s); kb, kilobase pair(s).

the large degree of nucleotide identity among the G-protein α-subunits within their respective open reading frame regions. This prompted us to look for unique target sequences within the 5′- and 3′-untranslated regions of the $G\alpha_q$ mRNA. The 36 nucleotides immediately upstream of and including the translation initiation codon were chosen to serve as the antisense target sequence. This 39-base pair sequence (5′-CGCGC-CGGCGGGGCTGCAGCGAGGCACTTCGGAAGAATG-3′) did not show any significant homology with sequences present in the GenBank™ data base, including $G\alpha_{11}$ (33% homology) and $G\alpha_{14}$ (27% homology).

Cell Culture and Transfection—FTO-2B cells were cultured in a 5% CO_2, 95% O_2 chamber and maintained in Ham's F-12/Dulbecco's modified Eagle's medium (1:1) supplemented with 10% fetal bovine serum. Cells were cotransfected with a plasmid that would allow for neomycin selection of positive transfectant clones. The control vector or pPCK-ASGα_q construct was added in 5-fold excess relative to the plasmid containing the selectable marker. Transfection was carried out using the Lipofectin reagent (Life Technologies, Inc.) according to the manufacturer's protocol.

Detection of Antisense RNA Expression—Total RNA was extracted as described previously (4). One microgram of total RNA was reverse transcribed using a pPCK-ASGa_q-specific downstream primer and then PCR-amplified in the presence of both the upstream and downstream primer set according to the manufacturer's protocol (Perkin-Elmer). The sequences for the upstream and downstream primers were dCGTTTAGTGAACCGTCAGA and dAGGTGGGGTCTTTCATTCCC, respectively.

Production of Transgenic Mice—Transgenic lines of mice were produced at the Transgenic Mouse Facility at SUNY Stony Brook using standard techniques (5, 6). Briefly the pPCK-ASGα_q construct was excised free of vector sequences and purified prior to microinjection into single-cell preimplantation embryos. Microinjected embryos were then transferred to pseudopregnant females. Offspring carrying the transgene were identified by PCR amplification and subsequent Southern analysis using a pPCK-ASGα_q-specific probe uniformly labeled with [^{32}P]dCTP (5). Five separate founder lines were identified by Southern analysis and bred over 10 generations (5).

White Adipocyte Isolation—White adipocytes were isolated from epididymal and parametrial fat pads by collagenase digestion, as described previously (5). Briefly, 0.5–1.0 g of adipose tissue was excised from male and female mice, weighed, and added to an equal volume of Krebs-Ringer phosphate buffer (KRP) containing 3% bovine serum albumin (KRP/BSA), prewarmed to 37 °C. The tissue was digested for 1 h using collagenase (1 mg/ml) at 37 °C in an orbital, shaking water bath. The isolated adipocytes were washed twice with the KRP/BSA buffer and then resuspended to a final volume to achieve 62.5 mg of wet weight of packed adipocytes/ml in the same buffer. The KRP/BSA buffer was supplemented with adenosine deaminase at a concentration of 0.5 unit/ml.

Cyclic AMP Accumulation and Lipolysis—Briefly, collagenase-digested white fat cells from epididymal and epoophoronal pads were incubated at 37 °C in KRP buffer supplemented with 3% bovine serum albumin and adenosine deaminase (0.5 unit/ml) for 30 min in the absence or presence of the drugs indicated. For lipolysis determinations, the assays were terminated with 0.65 N $HClO_4$. Samples were deproteinized and neutralized with KOH/KCl/imidazole (2.6/0.52/0.52 M, respectively) and the glycerol content determined by measuring the reduction of NAD^+ to NADH in a coupled assay. NADH production was assayed using a microplate fluorometer set to an excitation wavelength of 360 nm and an emission wavelength detection of 460 nm. The mass of glycerol per sample was extrapolated from a standard curve of stock glycerol. Cyclic AMP accumulation was measured using a competitive binding assay. Briefly, 80 μl of fat cells (~5 mg/tube) were treated with various agents for 6 min at 37 °C. The reaction was stopped by the addition of HCl (0.1 N final) and boiling for 1 min. The samples were neutralized with NaOH and assayed for cyclic AMP content. Cyclic AMP accumulation was measured in adipocytes stimulated with either phenylephrine, epinephrine, norepinephrine, or isoproterenol The data are expressed as the mean values in picomoles of cyclic AMP (±S.E.) per million cells from three independent trials, each performed in triplicate.

IP_3 and 1,2-sn-Diacyglycerol (DAG) Accumulation—Cells were incubated with the indicated agents and the IP_3 measured as described previously (21). DAG was determined using the DAG kinase assay (10). The data are expressed as the mean values in nanomoles (±S.E.) per million cells from three independent trials, each performed in triplicate.

G-protein Immunoblot Analysis—Membrane fractions were prepared from rat hepatoma FTO-2B cells, as described previously (5). Cell membranes were prepared from adipose tissue of transgenic mice and their control littermates (5). Aliquots of cell membrane were subjected to SDS-polyacrylamide (10% acrylamide) gel electrophoresis, and the separated proteins were transferred to nitrocellulose blots. The blots of the membrane proteins were probed with anti-peptide antibodies specific for $G\alpha_q$ (antibodies E973 and E976), $G\alpha_{i2}$ (antibody CM112), $G\alpha_s$ (antibody CM129), $G\beta_2$ (antibody CM162), $G\alpha_{11}$ (antibody E976), or $G\alpha_{i3}$ (antibody EC2), and the immune complexes were made visible by staining with a calf alkaline phosphatase-conjugated, goat anti-rabbit IgG second antibody (4, 5). The "CM" antibodies were prepared by our laboratory (4, 5).

RESULTS AND DISCUSSION

Defining the role of a specific G-protein subunit, like $G\alpha_q$, *in vivo* is a formidable task. We adopted the strategy of conditional, antisense RNA to ablate $G\alpha_q$ *in vivo* in a tissue-specific manner, creating loss-of-function mutants in adipose and liver, prominent sites of $G\alpha_q$ expression. The degree of nucleotide identity among the G-protein α-subunits within the open reading frames dictated selection of the 5′-untranslated region immediately upstream and including the ATG initiator codon (−33 to +3) as the antisense RNA sequence targeting Ga_q (Fig. 1). This region is unique with respect to sequences with the GenBank™ data base and does not share significant homology with other G-protein α-subunits (Fig. 1*A*), including other members of the G_q family, $G\alpha_{11}$ (33% homology with respect to $G\alpha_q$) and $G\alpha_{14}$ (27% homology with respect to $G\alpha_q$). A double-stranded oligodeoxynucleotide fragment antisense to $G\alpha_q$ was inserted into *Bcl*I and *Sal*I sites of the pPCK-AS vector (Fig. 1*B*), an inducible expression vector driven by the promoter of the PEPCK gene (5, 6). Screening of FTO-2B hepatoma cells stably transfected with pPCK-ASGα_q was performed from day 0 to day 12 following induction of the promoter with the chlorophenylthio analogue of cyclic AMP (CPT-cyclic AMP, 25 μM). Immunoblots reveal that levels of $G\alpha_{i2}$, $G\alpha_s$, and $G\beta_2$ were unaffected by induction of pPCK-ASGα_q, while staining with an antibody to $G\alpha_q$ displayed a 54% loss by day 6, and 86% loss of $G\alpha_q$ by day 9 following induction (Fig. 1*C*). By day 12 of the induction with CPT-cyclic AMP, $G\alpha_q$ was not detectable in the immunoblots of FTO-2B cell membranes. Induction of the pPCK-SGα_q vector, harboring the sense as compared to antisense sequence for $G\alpha_q$, resulted in a null phenotype, *i.e.* $G\alpha_q$ expression was normal. $G\alpha_q$ activates PLC-β in the liver (12–16) and suppression of $G\alpha_q$ in FTO-2B hepatoma cells reduced basal PLC activity from 2.7 ± 0.6 to 1.0 ± 0.3 ($p \leq 0.05$ for difference) and abolished PLC stimulation in response to either 10 nM angiotensin II (0.9 ± 0.3) or 10 μM norepinephrine (0.95 ± 0.2), as determined by mass assay of intracellular IP_3 accumulation at 30 s following hormonal stimulation ($n = 5$, pmol of IP_3 accumulation/μg of cellular protein).

The pPCK-ASGα_q construct was excised as a 7.0-kb *Eco*RI-*Bam*HI fragment, microinjected into single cell, preimplantation embryos, and the microinjected embryos were transferred into pseudopregnant recipients. BDF1 mice harboring the transgene were identified by PCR of tail DNA. Five independent founders were identified from two rounds of microinjection and implantation. Five separate founder lines have been propagated for more than 10 generations. Immunoblots of crude membranes from fat, liver, brain, and lung subjected to SDS-PAGE and stained with a $G\alpha_q$-specific antiserum reveal the near absence of $G\alpha_q$ in the tissues, fat and liver, targeted by the transgene (Fig. 1*D*). Immunoblots of brain and lung, tissues not targeted by the PEPCK vector, displayed normal levels of $G\alpha_q$ (Fig. 1*E*). Expression of $G\alpha_{i2}$, $G\beta_2$, and $G\alpha_{11}$ (not shown) were not significantly altered in the transgenic mice.

Necropsy and histology of the transgenic mice were performed. Prominent was the increase in body weight observed in the mice harboring the pPCK-ASGα_q transgene (Fig. 2*A*). By 5 weeks of age, the transgenic mice were >135% of the body weight of their control littermates, for both male and female

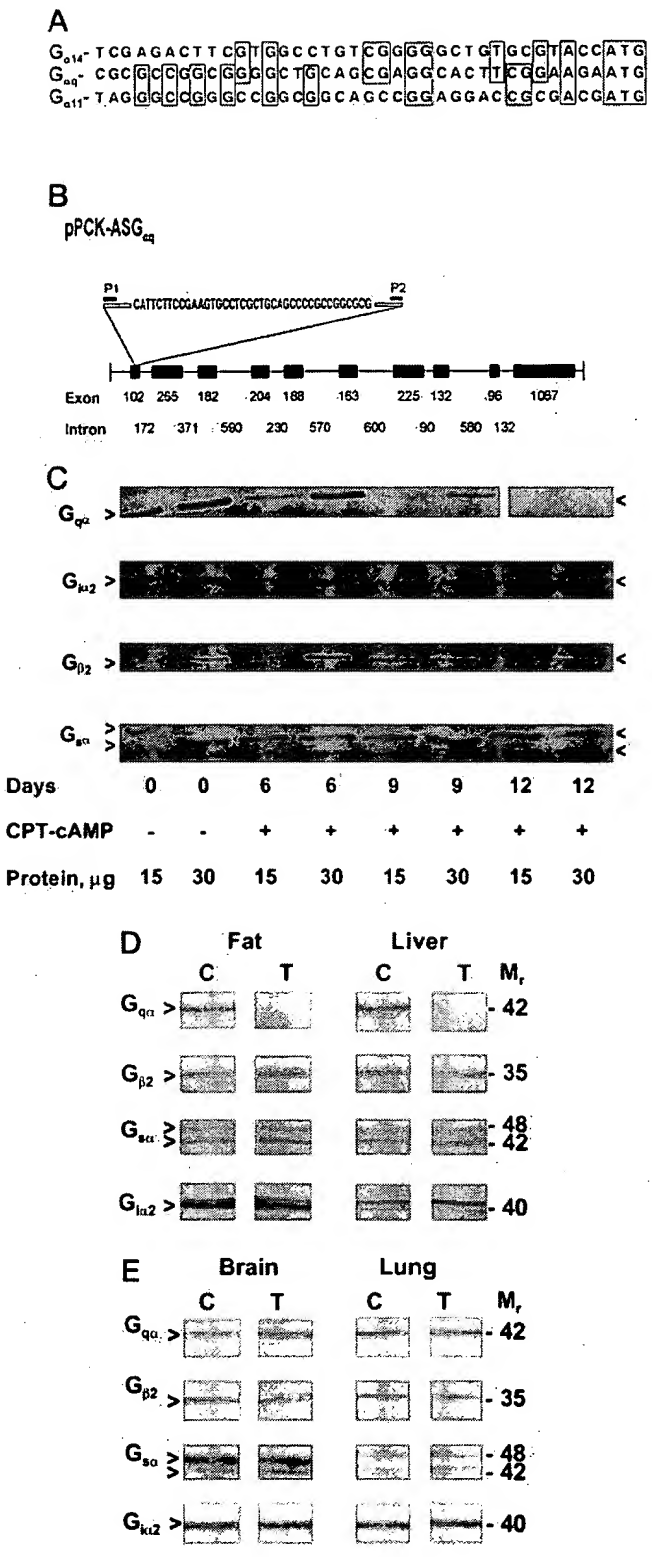

FIG. 1. **$G\alpha_q$ expression is suppressed in hepatoma cell stably transfected with pPCK-ASGα_q and in mice harboring the pPCK-ASGα_q transgene.** Comparison of the 5′-untranslated region from $G\alpha_q$ (nucleotides −33 to +3) with $G\alpha_{14}$ and $G\alpha_{11}$, additional members of the G_q family (*panel A*). The pPCK-ASGα_q construct for inducible expression of RNA antisense to $G\alpha_q$ (*panel B*). The 36-nucleotide sequence upstream of and including the translation initiation codon was inserted into the first exon of the rat phosphoenolpyruvate carboxykinase gene (*PCK*) to provide a 2.8-kb hybrid pPCK-ASGα_q antisense RNA, driven by a promoter which is silent *in utero* and activated at birth. Crude membranes (0.2 mg of protein/SDS-polyacrylamide gel electrophoresis lane) were prepared from rat hepatoma FTO-2B cells that were stably transfected with the pPCK-ASGα_q construct and induced with CPT-cyclic AMP for 0, 6, 9, and 12 days, subjected to SDS-polyacrylamide gel electrophoresis, transferred to nitrocellulose blots, and probed with rabbit polyclonal antisera specific for the G-protein subunits indicated (5, 6). Immunecomplexes were made visible with goat anti-rabbit IgG coupled to calf alkaline phosphatase and colorimetric development (*panel C*). Crude membranes were prepared from epididymal and epoophoronal white fat and liver (*panel D*) and brain and lung (*panel E*) tissues obtained from 24-week-old control (*C*) and transgenic (*T*) mice. Samples (15 μg of protein/lane) were subjected to SDS-polyacrylamide gel electrophoresis on a mini-gel apparatus and transferred to nitrocellulose for immunoblot analysis of various G-protein subunits, as described earlier (5, 6). For immunoblotting, the sample loading was limited to 15 μg/lane, within the range established for linearity between sample loading and quantification of immunostaining (not shown). Quantification of the blots revealed no significant change in the G-protein subunits tested between control and transgenic mouse tissues, with the exception of the loss of $G\alpha_q$ in liver and fat tissues. Expression of $G\alpha_s$ was normal in liver and fat, although reduced (<15%) occasionally in fat, but not liver, of some transgenic mice (not shown). Scanning densitometry values for immunoblots of fat tissue from control and transgenic mice, respectively, were as follows: $G\alpha_q$, 0.26, 0.01; $G\alpha_s$, 0.92, 0.88; $G\beta$, 0.31, 0.33; and $G\alpha_{i2}$, 0.72, 0.75 arbitrary OD units. Scanning densitometry values for immunoblots of liver tissue from control and transgenic mice, respectively, were as follows: $G\alpha_q$, 0.51; 0.02; $G\alpha_s$, 0.68, 0.64; $G\beta$, 0.27, 0.25; and $G\alpha_{i2}$, 0.22, 0.25 arbitrary OD units. Scanning densitometry of immunoblots from brain and lung revealed no significant differences in the values obtained with tissues from transgenic as compared to control mice (not shown). The antibodies employed for staining of immunoblots for specific G-proteins subunits were as follows: E973 for $G\alpha_q$; CM112 for $G\alpha_{i2}$; CM129 for $G\alpha_s$; E976 for $G\alpha_{11}$; and CM162 for $G\beta_2$.

mice alike (Fig. 2*B*). Progeny of the five founder lines harboring the transgene all display the increased body weight (not shown). The fat mass at 4 weeks after birth increased by 50% in the transgenic mice (Fig. 2*C*). At 8 weeks of age, the white epididymal and epoophoronal fat mass of the transgenic mice was 1.75-fold greater than that of the control mice. Segregated by gender for males, white fat mass (mg) was 215 ± 5 and 333 ± 8 ($n = 5, p \leq 0.05$) for 12-week-old control and transgenic mice, respectively. For females, white fat mass was 160 ± 10 mg and 303 ± 8 mg ($n = 6, p \leq 0.05$) for 12-week-old control and transgenic mice, respectively. By 24 weeks, the transgenic mice displayed a 1.4-fold increase in fat mass, and the percentage of whole body weight as fat mass was 2.3 ± 0.2 as compared to 1.1 ± 0.3 ($n = 6$) for control mice (Fig. 2*C*). Total body protein and nasal-anal length were unaffected by the presence of the transgene over this same range in age (not shown). Equally notable was the dramatic increase in adiposity, *i.e.* fat cell number, that occurred in the transgenic mice lacking $G\alpha_q$ expression in adipose tissue (Fig. 2*D*).

To assess the effects of $G\alpha_q$ deficiency on cell signaling, we investigated the adipocytes isolated from transgenic mice and their control littermates. PLC-β signaling by loss-of-function $G\alpha_q$-deficient white adipocytes was virtually abolished, *i.e.* IP_3 and DAG accumulation in response to norepinephrine, vasopressin, phenylephrine, or bradykinin (all hormones that activate PLC) was markedly attenuated (Fig. 3, *A* and *B*, respectively). Suppression of $G\alpha_q$ in adipocytes of the pPCK-ASGα_q mice and the stably transfected hepatoma cells abolished PLC activation by a variety of hormones (Figs. 1 and 3). This loss of signaling in $G\alpha_q$ deficiency occurs, although expression of the $G\alpha_{11}$ subunit was found to be normal (not shown). Both $G\alpha_q$ and $G\alpha_{11}$ are expressed in a number of tissues (12–14), including fat and liver. The observations from the present study suggest that $G\alpha_q$ and $G\alpha_{11}$ may not be redundant with respect to PLC activation *in vivo*.

Since PLC activation and accumulation of either IP_3 or DAG have not been implicated in controlling lipolysis, the pharmacology of the lipolytic response observed in the $G\alpha_q$-deficient adipocytes came as a great surprise (Fig. 3*C*). The lipolytic response to a mixed α- and β-adrenergic agonist norepineph-

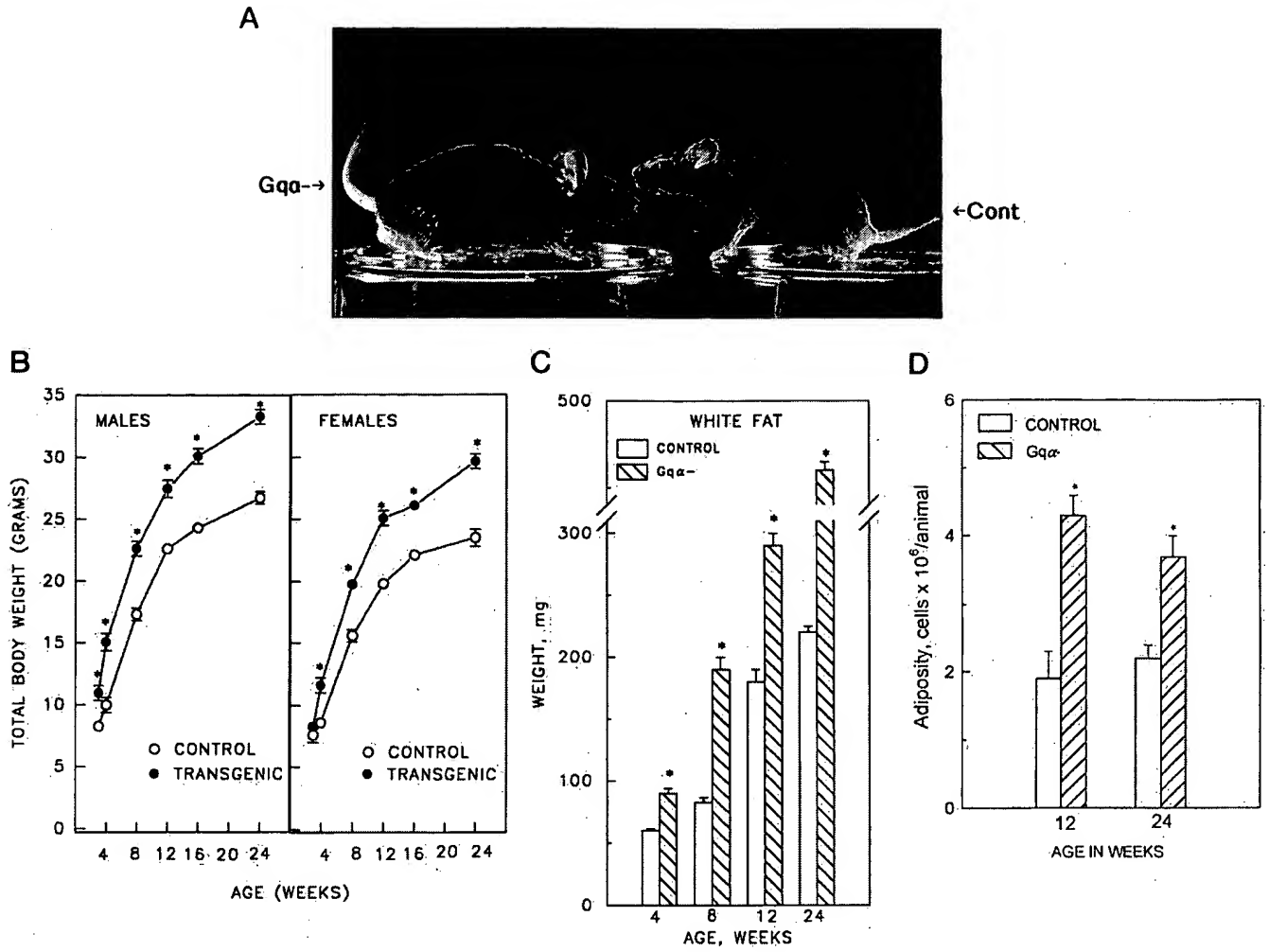

FIG. 2. **Suppression of $G\alpha_q$ expression by RNA antisense to $G\alpha_q$ causes increased body weight and fat mass.** The pPCK-ASGα_q transgenic mice have increased body weight (*panels A* and *B*), increased white fat mass (*panel C*), and increased adiposity (*panel D*). Five founders and the progeny of each of the founder lines for 10 generations were maintained and propagated by independent outbreeding to BDF1 control mice. The five founders and all members of their lineages at each generation display this phenotype (see Table I). In all cases, the data displayed were obtained from members of at least three of the five founder lines. Transgenic mice and their littermate controls were analyzed at ages spanning 3–24 weeks. The data are expressed as the mean values ± S.E. from at least six animals for each age group, transgenic and control alike. Fecundity and litter size were no different in the transgenic as compared to control mice. Mice shown in *panel A* were 12-week-old males, *left-hand panel*, transgenic mouse and *right-hand panel*, control mouse. *Panel B*, the body weight of pPCK-ASGα_q transgenic mice and their control littermates, segregated by sex. *Panel C*, the fat pad mass of pPCK-ASGα_q transgenic mice and their control littermates, pooled from male and female mice at the ages indicated for the sake of simplicity. Pair-feeding of the animals did not diminish the obese character of the transgenic mice. Nose-to-anus dimensions were not altered in the transgenic as compared to control mice. Adiposity was measured by determining the total white fat cell number from collagenase-digested, isolated epididymal and epoophoronal fat pads of single transgenic mice and paired, littermate controls, by cell counting using a hemocytometer. Throughout this work, statistical analysis was performed using the Student's *t* test. An *asterisk* denotes statistical significance with $p \leq 0.05$ for the difference between the mean values for transgenic ($G\alpha_q$-deficient) as compared to control mice.

rine was blunted in the $G\alpha_q$-deficient adipocytes. Lipolysis in response to the β-adrenergic agonist isoprenaline was impaired, whereas the response to the α_1-adrenergic agonist phenylephrine was abolished in the loss-of-function mutant cells. These results were unexpected, since neither a direct role of $G\alpha_q$ in activating adenylyl cyclase nor the existence of a prominent α_1-adrenergic stimulation of lipolysis have been reported. Analysis of cyclic AMP accumulation provided direct proof linking loss of $G\alpha_q$ to impaired lipolysis in response to β-adrenergic stimulation (acting via adenylyl cyclase) as well as to α_1-adrenergic stimulation (acting via PLC). Forskolin (10 μM)-stimulated cyclic AMP accumulation, in contrast, was actually elevated in the $G\alpha_q$-deficient as compared to control adipocytes (125 ± 15 and 160 ± 5 pmol/10^6 cells, respectively). Forskolin (10 μM)-stimulated lipolysis was equivalent in transgenic and control mice (14.1 ± 2.9 and 13.9 ± 0.8 μmol of glycerol release/10^6 cells, respectively), as were the abundance of β-adrenergic receptors (140 ± 4 and 133 ± 9 fmol/mg of protein, respectively) in crude adipocyte membranes and the amounts of cyclic AMP phosphodiesterase activity (1.33 ± 0.02 and 1.32 ± 0.09 pmol/min/mg of protein, respectively) in extracts of whole fat pads.

In the $G\alpha_q$-deficient cells, the impaired lipolytic response stimulated by norepinephrine was sensitive to the strict β-adrenergic antagonist propranolol, reflecting a residual β-adrenergic, cyclic AMP-mediated response (Fig. 4*A*). Adipocytes from control mice display sensitivity to both propranolol and the α_1-adrenergic antagonist prazosin. The former reflects the β-adrenergic response acting via cyclic AMP, while the latter reflects this newly discovered α_1-adrenergic response first detected through its loss in the $G\alpha_q$-deficient cells. Vasopressin (1 μM), which activates PLC, also stimulated lipolysis in adipocytes from control mice 1.8-fold over basal. The α_1-adrenergic stimulation of lipolysis was abolished by prazosin, but not by

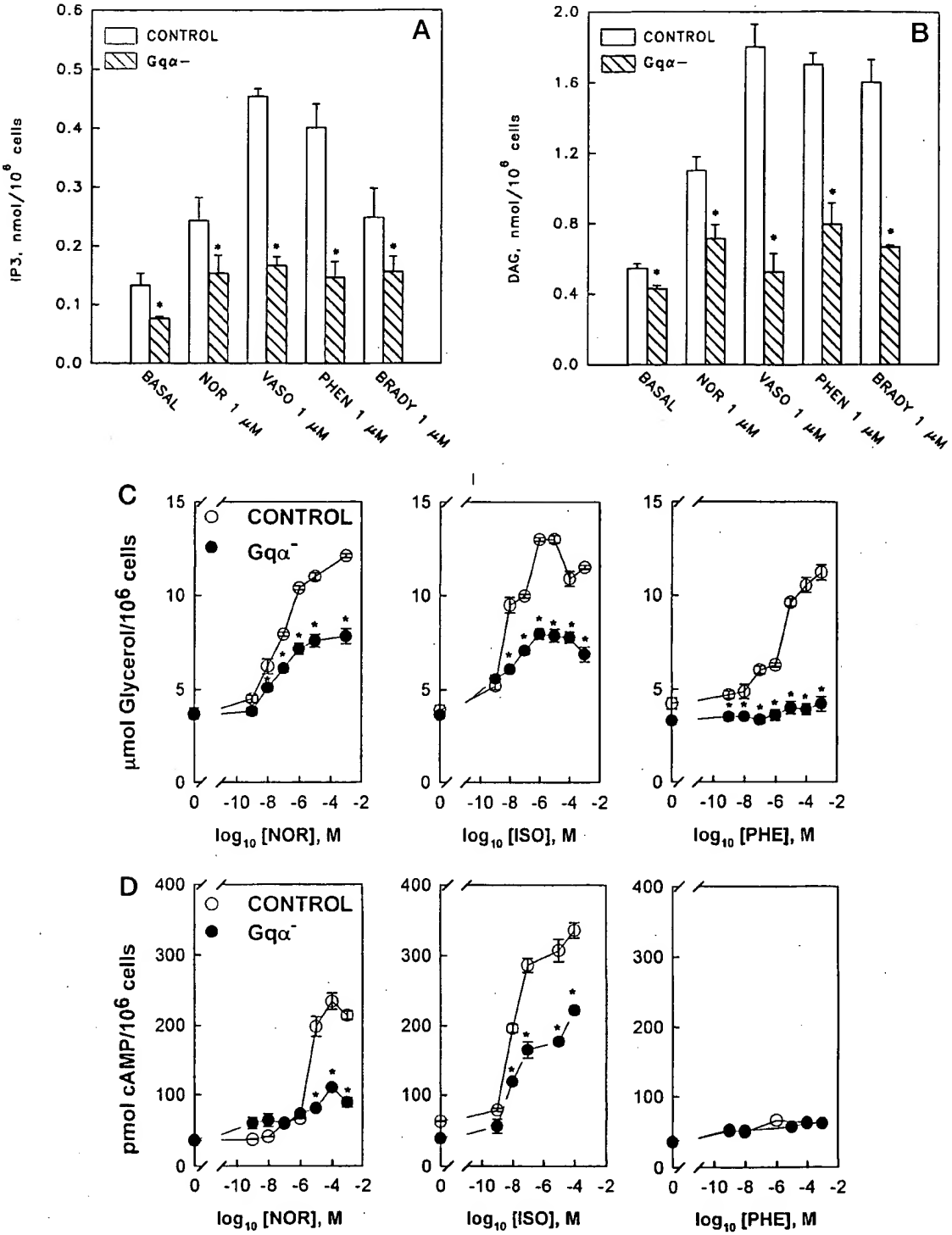

FIG. 3. **Adipocytes from pPCK-ASGα_q transgenic mice display loss-of-function with respect to activation of PLC and α_1-adrenergic regulation of lipolysis.** White adipocytes were isolated from epididymal and epoophoronal fat of transgenic mice and control littermates by collagenase digestion. Accumulation of IP_3 (*panel A*) and DAG (*panel B*) at 30 s following stimulation by 1 μM agonist (*NOR*, norepinephrine; *VASO*, vasopressin; *PHEN*, phenylephrine; *BRADY*, bradykinin) were measured in cells from mice 18–24 weeks of age. Intracellular IP_3 accumulation was measured by the mass assay employing the rabbit cerebellar IP_3-binding protein. DAG was assayed using a DAG kinase assay followed by thin-layer chromatographic separation of radiolabeled phosphate generated by the reaction. The DAG mass was calculated from a standard curve using authentic DAG. Lipolysis (*panel C*) and cyclic AMP accumulation (*panel D*) were measured in cells isolated from transgenic and control mice. The cells were challenged with varying concentrations of the mixed α- and β-adrenergic agonist norepinephrine (*NOR*), the β-adrenergic agonist isoprenaline (*ISO*), or the α-adrenergic agonist phenylephrine (*PHEN*) for 15 min (cyclic AMP accumulation) or 60 min (lipolysis via glycerol release). For cyclic AMP determinations, the assays were terminated at 15 min, and the accumulation of intracellular cyclic AMP measured using a competitive binding assay with bovine adrenal cyclic AMP binding protein. The data presented are mean values ± S.E. from at least three separate experiments, each performed on separate occasions. An *asterisk* denotes statistical significance with $p \leq 0.05$ for the difference between the mean values for transgenic ($G\alpha_q$-deficient) as compared to control mice.

propranolol (Fig. 4*B*). The loss-of-function $G\alpha_q$-deficient cells, in contrast, have essentially lost the lipolytic response to phenylephrine stimulation.

Although $G\alpha_q$ is not known to regulate adenylyl cyclase directly, the loss-of-function $G\alpha_q$ mutants displayed impaired β-adrenergic stimulation of cyclic AMP accumulation and lipol-

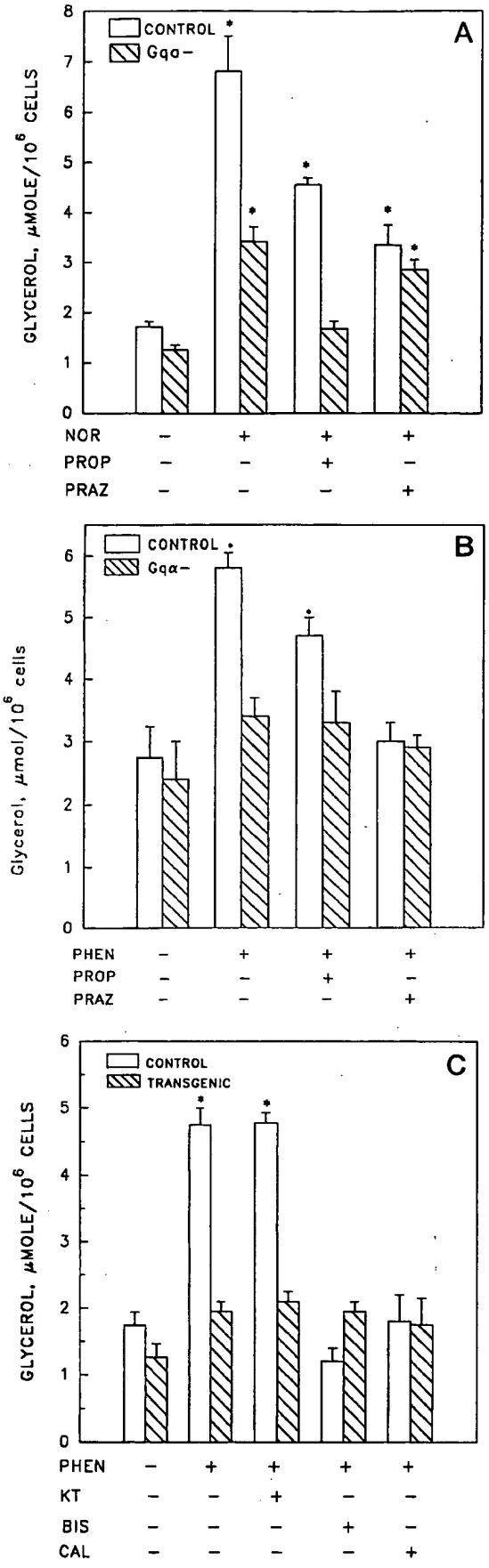

FIG. 4. **The pharmacology of the adrenergic lipolytic response reveals the existence of an α_1-adrenergic stimulatory pathway, absent in the $G\alpha_q$-deficient loss-of-function mutants.** White adipocytes were isolated from transgenic mice and their control littermates for study of the lipolytic response to adrenergic agonists. The lipolytic response was measured as described in the legend to Fig. 3. Stimulation of lipolysis by either 10 μM norepinephrine (*NOR*, *panel A*) or 10 μM phenylephrine (*PHEN*, *panels B* and *C*) was analyzed in the absence and presence of either the β-adrenergic antagonist propranolol (*PROP*, 10 μM) or the α_1-adrenergic antagonist prazosin (*PRAZ*, 1 μM). Inhibitors of protein kinase A (*KT*, KT5702, 1 μM) and protein kinase C (*BIS*, bis-indolylmaleimide, 1 μM; *CAL*, calphostin C, 100 nM) were examined for their ability to block the α_1-adrenergic stimulation of lipolysis in adipocytes from transgenic mice and their control littermates (*panel C*). The results are mean values ± S.E. from three to five separate experiments for each. An *asterisk* denotes statistical significance with $p \leq 0.05$ for the differences from mean basal values obtained with adipocytes isolated from both transgenic ($G\alpha_q$-deficient) and control mice.

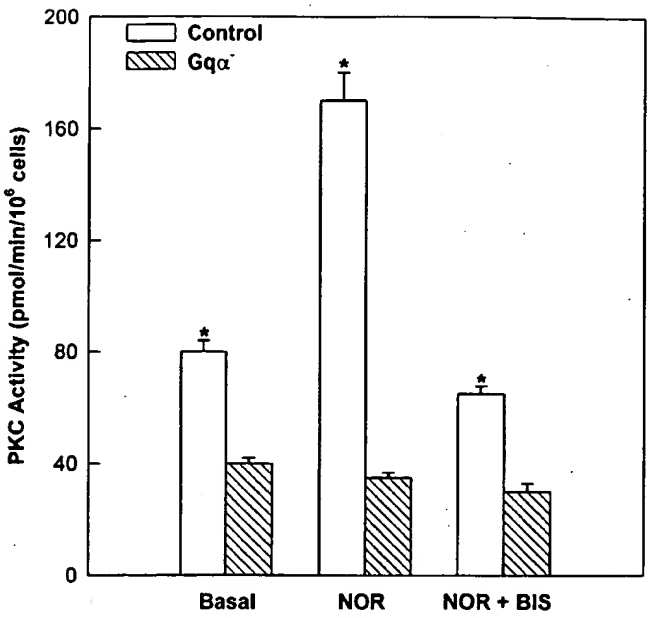

FIG. 5. **Adipocytes from pPCK-ASGα_q transgenic mice display loss of function with respect to activation of protein kinase C following challenge with norepinephrine.** White adipocytes were isolated from epididymal and epoophoronal fat of transgenic mice and control littermates by collagenase digestion. The activity of protein kinase C was measured in cells from mice 18–24 weeks of age. The cells were challenged for 5 min without (*Basal*) and with 10 μM of the mixed α- and β-adrenergic agonist norepinephrine (*NOR*), in the absence or presence of 0.1 mM bis-indolylmaleimide (*NOR + BIS*), a potent protein kinase inhibitor. Protein kinase C activity was measured in DEAE-cellulose-purified cell homogenates, as described elsewhere (30). The data presented are mean values ± S.E. from at least three separate experiments, each performed on separate occasions. An *asterisk* denotes statistical significance with $p \leq 0.05$ for the difference between the mean values for transgenic ($G\alpha_q$-deficient) as compared to control mice.

ysis. $G\alpha_q$, acting via PLC to promote IP_3 and DAG accumulation, may augment the cyclic AMP response indirectly, perhaps via effects on calcium- or protein kinase C-sensitive forms of adenylyl cyclase (22–25). We tested the role of protein kinase C using bis-indolylmaleimide and calphostin C, selective inhibitors of protein kinase C (Fig. 4*C*). Both calphostin C (100 nM) and bis-indolylmaleimide (1 μM) abolished the α_1-adrenergic stimulation of lipolysis, whereas the protein kinase A inhibitor KT-5720 (1 μM) was without effect. At 100 nM, bis-indolylmaleimide effectively blocked phenylephrine (10 μM)-stimulated lipolysis in adipocytes from control mice; glycerol release (μmol/10^6 cells), in response to this α_1-adrenergic agonist, declined from 4.7 to 1.2 in the absence *versus* presence of this protein kinase C inhibitor. The K_I for nonselective inhibition of protein kinase A by bis-indolylmaleimide is >2 μM (26). Since the protein kinase A inhibitor KT-5720 itself was without effect, nonselective effects of protein kinase C inhibitors, if they indeed occurred at these lower concentrations, would be irrelevant.

Measurement of protein kinase C activity in DEAE-cellulose-purified homogenates of cells challenged with and without norepinephrine was performed using adipocytes from the control and transgenic mice (Fig. 5). In adipocytes from control mice, norepinephrine stimulates protein kinase C activity, an action blocked by the addition of bis-indolylmaleimide. Suppression of $G\alpha_q$ in adipocytes of the pPCK-ASGα_q mice results in a frank reduction in protein kinase C activity in the basal state and a loss of norepinephrine-induced activation of protein kinase C. Total protein kinase activities for adipocytes from control and transgenic mice are equivalent, 310 ± 20 and 315 ± 18 pmol/min/million cells, respectively. Thus, α_1-adrenergic control of lipolysis is shown to be mediated via protein kinase C, a pathway revealed by its absence in the $G\alpha_q$-deficient state.

The absence of $G\alpha_q$ resulted in increased fat accumulation and hyperadiposity, observed within 5 weeks of age and sustained through adult life. Obesity has been reported in transgenic mice after genetic ablation of brown adipose tissue (27), supporting the role of this specialized tissue in preventing obesity (28). The pPCK-ASGα_q transgene was not expressed in brown adipose tissue (not shown). Expression of $G\alpha_q$, the uncoupling protein UCP, and the mRNAs for both were equivalent in brown adipose tissue from transgenic and control mice (not shown), suggesting no involvement of brown adipose tissue in enhanced fat accumulation by the pPCK-ASGα_q-expressing mice.

The absence of $G\alpha_q$ abolished an important stimulatory control of lipolysis, apparently predisposing the mice to accumulation of fat. Recently, G-proteins have been shown to play prominent roles in differentiation (2, 3) and neonatal growth (4–6). For progression of F9 teratocarcinoma cells to primitive endoderm (4) and for development of nerve growth cones (3), G-proteins appear to be acting directly or indirectly via protein kinase C (10, 29). In the present study we demonstrate the key role of PLC and protein kinase C in adipocyte signaling in the mature cells. The basis for the hyperadiposity in the cells deficient in $G\alpha_q$, however, remains to be established, but may reflect a critical role of $G\alpha_q$ in controlling adipogenic conversion *in vivo*.

Acknowledgments—We thank Dr. John H. Exton (HHMI, Vanderbilt University, Nashville, TN) for the generous gift of antibodies E973 and E976. We thank Dr. Jean Himms-Hagen (University of Ottawa, Ontario, Canada) for the generous gift of antibodies to UCP.

REFERENCES

1. Gilman, A. G. (1987) *Annu. Rev. Biochem.* **56,** 615–649
2. Wang, H.-y, Watkins, D. C., and Malbon, C. C. (1992) *Nature* **358,** 334–337
3. Strittmatter, S. M., Valenzuela, D., Kennedy, T. E., Neer, E. J., and Fishman, M. C. (1993) *Science* **259,** 77–79
4. Watkins, D. C., Johnson, G. L., and Malbon, C. C. (1992) *Science* **258,** 1373–1375
5. Moxham, C. M., Hod, Y., and Malbon, C. C. (1993) *Science* **260,** 991–995
6. Moxham, C. M., Hod, Y., and Malbon, C. C. (1993) *Dev. Genet.* **14,** 266–273
7. Bourne, H. R., Sanders, D. A., and McCormick, F. (1990) *Nature* **348,** 125–132
8. Igarashi, M., Strittmatter, S. M., Vartanian, T., and Fishman, M. C. (1993) *Science* **259,** 77–79
9. Strittmatter, S. M., Fishman, M. C., and Zhu, X. P. (1994) *J. Neurosci.* **14,** 2327–2338
10. Gao, P., and Malbon, C. C. (1996) *J. Biol. Chem.* **271,** 9002–9008
11. Rudolph, U., Finegold, M. J., Rich, S. S., Harriman, G. R., Srinivasan, Y., Brabet, P., Boulay, G., Bradley, A., and Birnbaumer, L. (1995) *Nat. Genet.* **10,** 143–150
12. Moxham, C. M., and Malbon, C. C. (1996) *Nature* **379,** 840–845
13. Taylor, S. J., Smith, J. A., and Exton, J. H. (1990) *J. Biol. Chem.* **265,** 17150–17156
14. Taylor, S. J. Choe, H. Z., Rhee, S. G., and Exton, J. H. (1991) *Nature* **350,** 516–518
15. Smrcka, A. V., Hepler, J. R., Brown, K. O., and Sternweis, P. C. (1991) *Science* **251,** 804–807
16. Waldo, G. L., Boyer, J. L., Morris, A. J., and Harden, T. K. (1991) *J. Biol. Chem.* **266,** 14217–14225
17. Hepler, J. R., Kozasa, T., Smrcka, A. V., Simon, M. I., Rhee, S. G., Sternweis, P. C., and Gilman, A. G. (1993) *J. Biol. Chem.* **268,** 14367–14375
18. LaMorte, V. J., Harootunian, A. T., Spiegel, A. M., Tsien, R. Y., and Feramisco, J. R. (1993) *J. Cell. Biol.* **121,** 91–99
19. Chien, K. R., Knowlton, K. U., Zhu, H., and Chien, S. (1991) *FASEB J.* **5,** 3037–3046
20. Kalinec, G., Nazarali, A. J., Hermouet, S., Xu, N., and Gutkind, J. S. (1992) *Mol. Cell. Biol.* **12,** 4687–4693
21. Watkins, D. C., Moxham, C. M., Morris, A. J., and Malbon, C. C. (1994) *Biochem. J.* **299,** 593–596
22. De Vivo, M., Chen, J., Codina, J., and Iyengar, R. (1992) *J. Biol. Chem.* **267,** 18263–18266
23. Kawabe, J., Iwami, G., Ebina, T., Ohno, S., Katada, T., Ueda, Y., Homcy, C. J., and Ishikawa, Y. (1994) *J. Biol. Chem.* **269,** 16554–16558
24. Jacobowitz, O., and Iyengar, R. (1994) *Proc. Natl. Acad. Sci. U. S. A.* **91,** 10630–10634
25. Taussig, R., and Gilman, A. G. (1995) *J. Biol. Chem.* **270,** 1–4
26. Toullec, D. Pianetti, P., Coste, H., Bellevergue, P., Grand-Perret, T., Ajakane, M., Baudet, V., Boisson, P., Boursier, E., Loriolle, F., Duhamel, L., Charon, D., and Kirilovsky, J. (1991) *J. Biol. Chem.* **266,** 15771–15781
27. Lowell, B. B., Susulic, V. S., Hamann, A., Lawitts, J. A., Himms-Hagen, J., Boyer, B. B., Kozak, L. P., and Flier, J. S. (1993) *Nature* **366,** 740–742
28. Himms-Hagen, J. (1989) *Proc. Lipid Res.* **28,** 67–115
29. Xie, R., Li, L., Goshima, Y., and Strittmatter, S. M. (1995) *Brain Res.* **87,** 77–86
30. Gao, P., and Malbon, C. C. (1996) *J. Biol. Chem.* **271,** 9002–9008

EXHIBIT J

THE JOURNAL OF BIOLOGICAL CHEMISTRY
Vol. 270, No. 14, Issue of April 7, pp. 8037–8043, 1995
Printed in U.S.A.

Expression of Antisense to DNA Methyltransferase mRNA Induces DNA Demethylation and Inhibits Tumorigenesis*

(Received for publication, October 10, 1994, and in revised form, January 24, 1995)

A. Robert MacLeod and Moshe Szyf‡

From the Department of Pharmacology and Therapeutics, McGill University, Montreal H3G 1Y6, Canada

Many tumor cell lines overexpress DNA methyltransferase (MeTase) activity; however it is still unclear whether this increase in DNA MeTase activity plays a causal role in naturally occurring tumors and cell lines, whether it is critical for the maintenance of transformed phenotypes, and whether inhibition of the DNA MeTase in tumor cells can reverse transformation. To address these basic questions, we transfected a murine adrenocortical tumor cell line Y1 with a chimeric construct expressing 600 base pairs from the 5′ of the DNA MeTase cDNA in the antisense orientation. The antisense transfectants show DNA demethylation, distinct morphological alterations, are inhibited in their ability to grow in an anchorage-independent manner, and exhibit decreased tumorigenicity in syngeneic mice. *Ex vivo*, cells expressing the antisense construct show increased serum requirements, decreased rate of growth, and induction of an apoptotic death program upon serum deprivation. 5-Azadeoxycytidine-treated cells exhibit a similar dose-dependent reversal of the transformed phenotype. These results support the hypothesis that the DNA MeTase is actively involved in oncogenic transformation.

Vertebrate DNA is methylated at the 5-position of the cytosine residues in the dinucleotide sequence CpG (1, 2). Twenty percent of the CpG sites are nonmethylated, and these sites are distributed in a nonrandom manner to generate a pattern of methylation that is site-, tissue-, and gene-specific (1–3). Methylation patterns are formed during development: establishment and maintenance of the appropriate pattern of methylation is critical for development (4) and for defining the differentiation state of a cell (5–7). The pattern of methylation is maintained by the DNA MeTase[1] at the time of replication (8), and the level of DNA MeTase activity and gene expression is regulated with the growth state of different primary (8) and immortal cell lines (9). This regulated expression of DNA MeTase has been suggested to be critical for preserving the pattern of methylation (8–10).

An activity that has a widespread impact on the genome such as DNA MeTase is a good candidate to play a critical role in cellular transformation. This hypothesis is supported by many lines of evidence that have demonstrated aberrations in the pattern of methylation in transformed cells. While many reports show hypomethylation of total genomic DNA (11) as well as individual genes in cancer cells (12), other reports have indicated that hypermethylation is an important characteristic of cancer cells (13). First, large regions of the genome such as CpG-rich islands (14) or regions in chromosomes 17p and 3p that are reduced to homozygosity in lung and colon cancer, respectively, are consistently hypermethylated (15, 16). Second, the 5′ region of the retinoblastoma (Rb) and Wilms Tumor (WT) genes are methylated in a subset of tumors, and it has been suggested that inactivation of these genes in the respective tumors resulted from methylation rather than a mutation (17). Third, the short arm of chromosome 11 is regionally hypermethylated in certain neoplastic cells (15). Several tumor suppressor genes are thought to be clustered in that area (18). If the level of DNA MeTase activity is critical for maintaining the pattern of methylation as has been suggested before (8–10), one possible explanation for this observed hypermethylation is the fact that DNA MeTase is dramatically induced in many tumor cells well beyond the change in the rate of DNA synthesis (13, 19). The observation that the DNA MeTase promoter bears AP-1 sites (20) and is activated by the Ras-AP-1 signaling pathway (21) is consistent with the hypothesis that elevation of DNA MeTase activity is an effect of activation of the Ras-Jun signaling pathway (22).

It has recently been demonstrated that forced expression of exogenous DNA MeTase cDNA causes transformation of NIH 3T3 cells supporting the hypothesis that overexpression of DNA MeTase can cause cellular transformation (23). The critical question that remains to be answered is whether indeed the level of expression of the endogenous DNA MeTase plays a causal role in tumors that are induced by naturally occurring oncogenic signal transduction pathways. To address this question, we have chosen the adrenocortical carcinoma cell line Y1 as a model system. Y1 is a cell line that is derived from a naturally occurring adrenocortical tumor in LAF1 mice (24). Y1 cells bear a 30–40-fold amplification of the *ras* proto-oncogene (25). If the level of expression of DNA MeTase activity is critical for the oncogenic state, then the transformed state of a cell should be reversed by partial inhibition of DNA methylation. We have previously demonstrated that forced expression of an "antisense" mRNA to the most 5′ 600 bp of the DNA MeTase message (pZαM) can induce limited DNA demethylation in 10T1/2 cells (7). To directly test the hypothesis that the tumorigenicity of Y1 cells is controlled by the DNA MeTase, we transfected either pZαM or a pZEM control into Y1 cells. We demonstrate that inhibition of DNA MeTase activity causes demethylation of Y1 DNA and results in reversal of the tumorigenic phenotype suggesting that DNA MeTase plays a critical role in tumorigenesis.

MATERIALS AND METHODS

Cell Culture and DNA-mediated Gene Transfer—Y1 cells were maintained as monolayers in F-10 medium which was supplemented with 7.25% heat-inactivated horse serum and 2.5% heat-inactivated fetal

* This paper was supported in part by a grant from the Cancer Research Society and the NCI (Canada). The costs of publication of this article were defrayed in part by the payment of page charges. This article must therefore be hereby marked "*advertisement*" in accordance with 18 U.S.C. Section 1734 solely to indicate this fact.

‡ Scientist of the National Cancer Institute (Canada). To whom correspondence and reprint requests should be addressed. Tel.: 514-398-7107; Fax: 514-398-6690; E-mail: mcms@musica.mcgill.ca.

[1] The abbreviations used are: MeTase, methyltransferase; 5-azaCdR, 5-azadeoxycytidine; bp, base pair(s); kb, kilobase pair(s); PCR, polymerase chain reaction.

calf serum (Immunocorp, Montreal) (23). 5-azaCdR was from Sigma, all other media and reagents for cell culture were obtained from Life Technologies, Inc. Y1 cells (1×10^6) were plated on a 150-mm dish (Nunc) 15 h before transfection. The pZαM expression vector (7) encoding the 5′ of the murine DNA methyltransferase cDNA (10 μg) was co-introduced into Y1 cells with 1 μg of pUCSVneo as a selectable marker by DNA-mediated gene transfer using the calcium phosphate protocol, and G418-resistant cells were cloned in selective medium (0.25 mg/ml G418) (26). Anchorage-independent growth in soft agar (1×10^3 cells) was as described previously (27).

DNA and RNA Analyses—Genomic DNA was prepared from pelleted nuclei, and total cellular RNA was prepared from cytosolic fractions according to standard protocols (26). *Msp*I or *Hpa*II restriction enzymes (Boehringer Mannheim) were added to DNA at a concentration of 2.5 units/μg for 8 h at 37 °C. At least three different DNA preparations isolated from three independent passages were assayed per transfectant. To quantify the relative abundance of DNA MeTase mRNA, total RNA (3 μg) was blotted onto Hybond N$^+$ using the Bio-Rad slot-blot apparatus. The filter-bound RNA was hybridized to a ^{32}P-labeled 1.31-kb cDNA probe encoding the putative catalytic domain of the mouse DNA MeTase (3170–4480) (28) and exposed to XAR film (Kodak). The relative amount of total RNA was determined by measuring the signal obtained after hybridization to an 18 S RNA-specific ^{32}P-labeled oligonucleotide (29). The autoradiograms were scanned with a Scanalytics scanner (one-dimensional analysis), and the signal at each band was determined and normalized to the amount of total RNA at the same point. Three determinations were performed per RNA sample.

Nearest Neighbor Analysis—Two μg of DNA were incubated at 37 °C for 15 min with 0.1 unit of DNase, 2.5 μl of [α-^{32}P]dGTP (3000 Ci/mmol from Amersham), 2 Kornberg units of DNA polymerase (Boehringer) were then added, and the reaction was incubated for an additional 25 min at 30 °C. Fifty μl of water were then added to the reaction mixture, and the nonincorporated nucleotides were removed by spinning through a Microspin S-300 HR column (Pharmacia). The labeled DNA (20 μl) was digested with 70 μg of micrococcal nuclease (Pharmacia) in the manufacturer's recommended buffer for 10 h at 37 °C. Equal amounts of radioactivity were loaded on TLC phosphocellulose plates (Merck), and the 3′ mononucleotides were separated by chromatography in one dimension (isobutyric acid:H_2O:NH_4OH in the ratio 66:33:1). The chromatograms were exposed to XAR film (Eastman-Kodak), and the autoradiograms were scanned by scanning laser densitometry (Scanalytics one-dimensional analysis). Spots corresponding to cytosine and 5-methylcytosine were quantified.

Assay of DNA MeTase Activity—To determine nuclear DNA MeTase levels, cells were maintained at a nonconfluent state and fed with fresh medium every 24 h for at least 3 days prior to harvesting, and DNA MeTase activity was assayed as described previously (9).

Strand-specific Reverse-transcribed PCR—Total RNA (1 μg) prepared from each transfectant was reverse-transcribed with either a sense primer corresponding to bases 1–30 in the published mouse DNA MeTase cDNA sequence (28), 5′ GCAAACAGAAATAAAAAGCCAGTTGTGTGA 3′ to detect antisense RNA or an antisense primer corresponding to bases 475–451, or 5′ CCACAGCAGCTGCAGCACCACTCT 3′ to detect sense DNA MeTase RNA using the conditions described above. RNA incubated with reverse transcriptase in the absence of primers was used as a control. The reaction was terminated by heating to 95 °C for 10 min. The reverse-transcribed cDNA was subjected to amplification in the presence of both primers using the Hot Tub amplification protocol conditions described above. The DNA was amplified for 40 cycles of 2 min at 95 °C, 2 min at 60 °C, and 0.5 min at 72 °C. The reaction products were separated on an agarose gel, Southern blotted onto Hybond N$^+$ filter, and hybridized with a ^{32}P-labeled internal oligonucleotide corresponding to bases 190–211: 5′ AAATGGCAGACTCAAATAGAT 3′. The conditions used (40 cycles of amplification) do not provide a quantitative assessment of the level of mRNA, but were used to exclude the possibility that small levels of antisense mRNA is present in the control transfectants.

Tumorigenicity Assays—LAF-1 mice (Bar Harbor) (6–8-week-old males) were injected subcutaneously (in the flank area) with 10^6 cells. Mice were monitored for the presence of tumors by daily palpation. Mice bearing tumors of greater than 1 cm in diameter were sacrificed, while tumor-free mice were kept for 90 days.

Electron Microscopy—Cells were fixed in glutaraldehyde (2.5%) in cacodylate buffer (0.1 M) for 1 h and further fixed in 1% osmium tetroxide. The samples were dehydrated in ascending alcohol concentrations and propylene oxide followed by embedding in Epon. Semithin sections (1 μm) were cut from blocks with an ultramicrotome and counterstained with uranyl acetate and lead citrate. Samples were analyzed using a Philips 410 electron microscope (30).

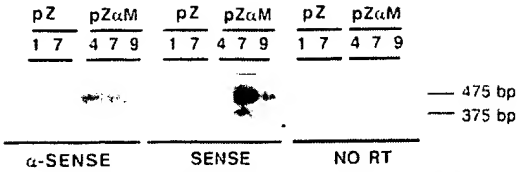

FIG. 1. **Expression of pZαM in Y1 adrenocortical cells.** To determine the strand specificity of the RNA transcribed by the pZαM vector, we employed a reverse transcriptase-PCR analysis using a sense-specific primer (*lanes labeled SENSE*), an antisense-specific primer (*lanes labeled α-SENSE*), or no primers (*lanes labeled NO RT*). Total RNA (1 μg) was reverse-transcribed with either a sense-specific primer, an α-sense-specific primer, or no primers. Resulting cDNA was then subjected to PCR with the complementary oligonucleotide (sense or α-sense) as described under "Materials and Methods," one-tenth of the PCR reaction was Southern-blotted and hybridized with a ^{32}P-labeled oligonucleotide encoding a sequence included in the amplified mRNA region (see "Materials and Methods" for description of the sequences of the primers). Sense DNA MeTase (*SENSE*) is observed in both pZαM and control pZEM transfectants as expected (475-bp product). An antisense transcript is seen only in pZαM transfectants. An unexpected additional sense amplification product of 375 bp is seen in all the pZαM transfectants.

RESULTS

Expression of Antisense to the DNA Methyltransferase mRNA in Y1 Cells Results in Limited Inhibition of DNA Methylation—To directly inhibit DNA methylation in Y1 cells, we introduced either the DNA MeTase antisense expression construct pZαM (encoding 600 bp from the 5′ of the DNA MeTase cDNA in the antisense orientation) or a pZEM control vector (7) into Y1 cells by DNA-mediated gene transfer as described under "Materials and Methods." Six G418-resistant colonies were isolated and propagated for both constructs. All antisense transfectants (determined by a preliminary Southern blot analysis) exhibited distinct morphological differences from the pZEM transfectants or nontransfected Y1 cells. Based on Northern blot analysis of the antisense mRNA expression, three independent pZαM transfectants (4, 7, 9) were selected for further characterization.

To verify that the antisense mRNA strand is transcribed in the pZαM transfectants, we employed reverse-transcribed PCR analysis using strand-specific primers as described under "Materials and Methods." The experiment presented in Fig. 1 demonstrates that when the sense oligonucleotide is used for reverse transcription (transcribing the antisense mRNA strand), the expected 0.475- kb amplification product is observed only in pZαM transfectants. As expected, the endogenous DNA MeTase sense mRNA is amplified in both pZEM and pZαM transfectants when the antisense oligonucleotide is used for reverse transcription (sense). Interestingly, a smaller amplification product (0.375 kb) is also seen in the pZαM lines suggesting that another splice variant of DNA MeTase mRNA is transcribed in these transfectants. The biological significance of the induction of the smaller variant in the pZαM transfectants is unclear.

The mechanism responsible for inhibition of gene expression by antisense is still unclear; however, some models suggest that degradation of the hybrid RNA by RNase H might be involved. To determine whether expression of an antisense to the DNA MeTase can lead to a reduction in the steady state level of endogenous DNA MeTase mRNA, we isolated total RNA from the antisense transfectants and the pZEM controls. DNA MeTase activity is regulated with the state of growth of cells (8, 9); therefore, all cultures were maintained at the logarithmic phase of growth and fed with fresh medium every 24 h for 3 days prior to harvesting. Total RNA isolated from the

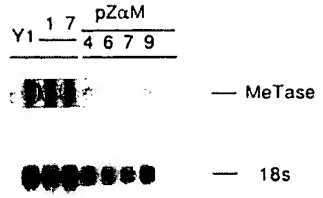

FIG. 2. **DNA MeTase expression, activity, and genomic methylation levels of pZαM transfectants.** Total cellular RNA (10 μg) prepared from pZαM lines (*4*, *6*, *7*, and *9*), pZEM transfectants (*1* and *7*) and from Y1 controls was subjected to Northern blot analysis and hybridization with a 1.3-kb DNA MeTase 3′-cDNA probe (encoding bases 3170–4480 from the cloned mouse cDNA (27)). The filter was stripped and rehybridized with an 18 S rRNA probe. Relative MeTase expression was determined by densitometric analysis (see text).

transfectants was subjected to a Northern blot analysis and sequentially hybridized with a probe to the putative catalytic domain of the mouse DNA MeTase mRNA (MET 3′) and an 18 S rRNA-specific ^{32}P-labeled oligonucleotide probe as described under "Materials and Methods." A result of such an analysis is presented in Fig. 2. Scanning of the autoradiogram indicates that the relative abundance of the 5-kb DNA MeTase mRNA (Fig. 2, *top panel*) relative to 18 S rRNA (Fig. 2, *bottom panel*) is reduced 2-fold in the three antisense transfectants. To quantify expression of DNA MeTase, the different RNA samples were subjected to a slot-blot analysis and sequential hybridization with the DNA MeTase and 18 S rRNA probes. The relative level of DNA MeTase mRNA in the different samples was determined by scanning densitometry. The results of such an analysis show that the pZαM transfectants exhibit an average decrease of 45% and a maximal decrease of 58% in the abundance of DNA MeTase mRNA relative to the pZEM controls ($p < 0.001$). The mean value for the control group was 0.480, S.D. = 0.104, the mean for the antisense group was 0.280, S.D. = 0.066.

We next compared the DNA MeTase enzymatic activity present in nuclear extracts prepared from antisense transfectants relative to control pZEM transfectants using *S*-[*methyl*-^{3}H]adenosyl-L-methionine as the methyl donor and a hemimethylated double-stranded oligonucleotide as a substrate. The results of two experiments with triplicate determinations each indicate that the three pZαM transfectants express a lower level of DNA MeTase activity than the control transfectants with an average inhibition of DNA MeTase activity of 42% and a maximum of 48% relative to control ($p < 0.05$).

Whereas our experiments demonstrate that the DNA MeTase antisense transfectants bear a lower level of DNA MeTase activity than the control transfectants, it is important to note that we measured only steady state levels in the transfectants. It is hard to assess the actual level of inhibition of DNA MeTase activity at the time of transfection, when a higher copy number of DNA MeTase antisense RNA might have been present in the cell. The steady state level of DNA MeTase mRNA might reflect an equilibrium of different cellular regulatory controls over the level of DNA MeTase activity in the cell. To directly demonstrate that expression of the DNA MeTase antisense leads to inhibition of DNA methylation activity in the cell, we determined whether it leads to a general reduction in the level of methylation of the genome. We performed a "nearest neighbor" analysis using [α-^{32}P]dGTP as described previously (6). This assay enables one to determine the percentage of methylated and nonmethylated cytosines residing in the dinucleotide sequence CpG (6). The results of three such experiments show that the mean value for the pZEM controls as a group was 9.7% nonmethylated cytosines, S.D. = 2.13, the mean value for the antisense lines as a group was 23.83% cytosine, S.D. = 5.88. $p < 0.001$.

In summary, our experiments demonstrate that expression of an antisense to the DNA MeTase mRNA leads to partial inhibition of DNA MeTase mRNA and DNA MeTase enzymatic activities and a significant reduction in the level of genomic cytosine methylation.

Demethylation of Specific Genes in Y1 and pZαM Transfectants—To further verify that expression of pZαM results in demethylation and to determine whether specific genes were demethylated, we resorted to a *Hpa*II/*Msp*I restriction enzyme analysis followed by Southern blotting and hybridization with specific gene probes. *Hpa*II cleaves the sequence CCGG, a subset of the CpG dinucleotide sequences, only when the site is unmethylated, while *Msp*I will cleave the same sequence irrespective of its state of methylation. By comparing the pattern of *Hpa*II cleavage of specific genes in cells expressing pZαM with that of the parental Y1 or cells harboring only the vector, we determined whether the genes are demethylated in the antisense transfectants. We first analyzed the state of methylation of the steroid 21-hydroxylase gene (C21) (29, 31). This gene is specifically expressed and hypomethylated in the adrenal cortex, but is inactivated and hypermethylated in Y1 cells (29, 31). We have previously suggested that hypermethylation of C21 in the Y1 cell is part of the transformation program that includes the shutdown of certain differentiated functions (29). DNA prepared from Y1, pZαM (4, 7, 9), and pZEM (1 and 7) transfectants was subjected to either *Msp*I or *Hpa*II digestion, Southern blot analysis, and hybridization with a 3.8-kb *Bam*HI fragment containing the body of the C21 gene and 3′ sequences (Fig. 3, *bottom panel*, for physical map). Full demethylation of this region should yield a doublet at ~1 kb, an 0.8-kb fragment, and a 0.4-kb fragment, as well as a number of low molecular weight fragments at 0.1–0.4 kb. As observed in Fig. 3, the C21 locus is heavily methylated in Y1 cells, as well as the control transfectant, as indicated by the high molecular weight fragments. Only a relatively weak digestion product is seen at 1.9 kb (Fig. 3). This pattern of hypermethylation of C21 which is observed in Y1 cells and different control transfectants, that were analyzed in our laboratory in the last 5 years, is markedly stable. On the other hand, the antisense transfectant's DNA is significantly hypomethylated at this locus as indicated by the relative diminution of the high molecular weight fragments and relative intensification of the partial fragment at 1.9 kb. The appearance of new partial fragments in the lower molecular weight range between 1 and 0.4 kb indicates partial hypomethylation at a large number of *Hpa*II sites contained in the 3′ region of the C21 gene (see physical map) (29, 31). The pattern of demethylation, indicated by the large number of partial *Hpa*II fragments, is compatible with a general partial hypomethylation rather than a specific loss of methylation in a distinct region of the C21 gene.

To determine whether demethylation is limited to genes that are potentially expressible in Y1 cells such as the adrenal cortex-specific C21 gene (29) or if the demethylation is widely spread in the genome, we tested the methylation state of the MyoD (32) and p53 5′ locus. Specific demethylation of MyoD and the p53 fragment was seen in the pZαM transfectants (data not shown).

Morphological Transformation Loss of Anchorage-independent Growth and Inhibition of Tumorigenicity of Y1 Cells Expressing Antisense to the DNA MeTase—As the level of DNA MeTase activity is regulated with the state of growth and is induced in transformed cells and in tumors *in vivo* (8, 9, 13, 19), we determined whether expression of the DNA MeTase antisense construct results in a change in the tumorigenic potential of Y1 cells. A comparison of pZαM transfectants and controls showed a small

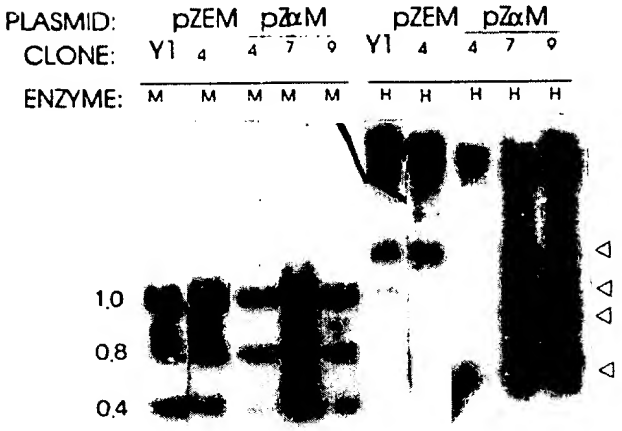

probe: C21 3.8

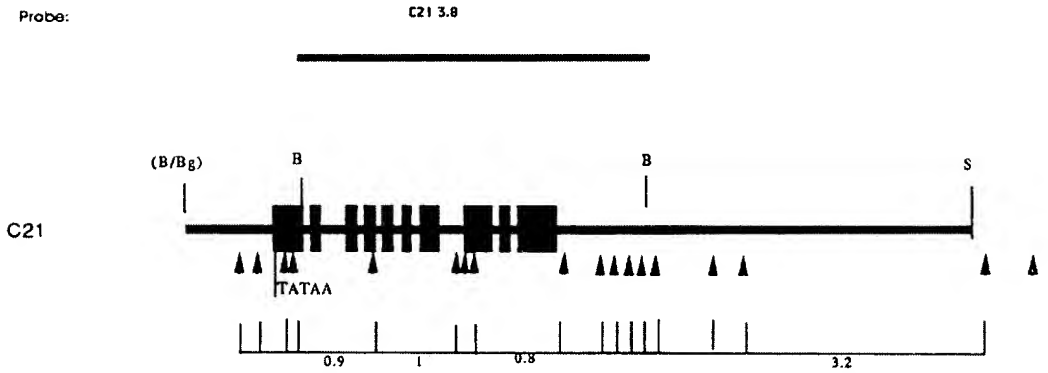

FIG. 3. **The pattern of methylation of C21 hydroxylase in pZαM transfectants and pZEM controls.** Genomic DNA (10 μg) was extracted from the transfected lines and subjected to digestion with either *Msp*I (*M*) or *Hpa*II (*H*), Southern blot transfer, and hybridization with a ^{32}P-labeled DNA probe (3.8-kb genomic fragment of the C21 gene, see *bottom panel* for physical map). The *open arrows* indicate *Hpa*II fragments resulting from demethylation of the different sites in the C21 gene in pZαM transfectants. Complete digestion of the region will yield 0.36- and 0.16-kb fragments.

but statistically significant reduction in the growth rate of antisense lines relative to the Y1 controls especially at higher densities (which is statistically significant, $p < 0.001$). This may reflect contact-inhibited growth and increased serum requirements of the antisense lines (data not shown). The morphological properties of the pZαM transfectants further support this conclusion (Fig. 4). While control Y1 and pZEM cells exhibit limited contact inhibition and form multilayer foci, pZαM transfectants exhibit a more rounded and distinct morphology and grow exclusively in monolayers, and, in many cases, pZαM cells form distinct cellular processes (Fig. 4).

The ability of cells to grow in an anchorage-independent fashion is considered to be an indicator of tumorigenicity (27). A soft agar assay performed in triplicate showed that the pZαM transfectants demonstrate a significant decrease in their ability to form colonies in soft agar: pZEM 1 and 7 form an average of 38 and 37 colonies, respectively, while pZαM transfectants 4, 7, and 9 formed an average of 12, 15, and 18 colonies, respectively. Moreover, the colonies that do form are significantly smaller and contain fewer cells.

Another indicator of the state of transformation of a cell is its serum dependence. Tumor cells exhibit limited dependence on serum and are usually capable of serum-independent growth (33). Factors present in the serum are essential for the survival

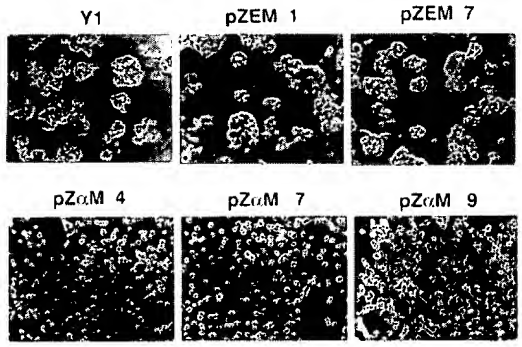

FIG. 4. **Morphological transformation of Y1 cells transfected with pZαM.** Phase contrast microscopy at × 200 magnification of living cultures of Y1 clonal transfectants with pZαM and pZEM controls. Equal numbers of cells were plated (1×10^5 cells per well in a six-well dish), and pictures were taken 72 h after seeding.

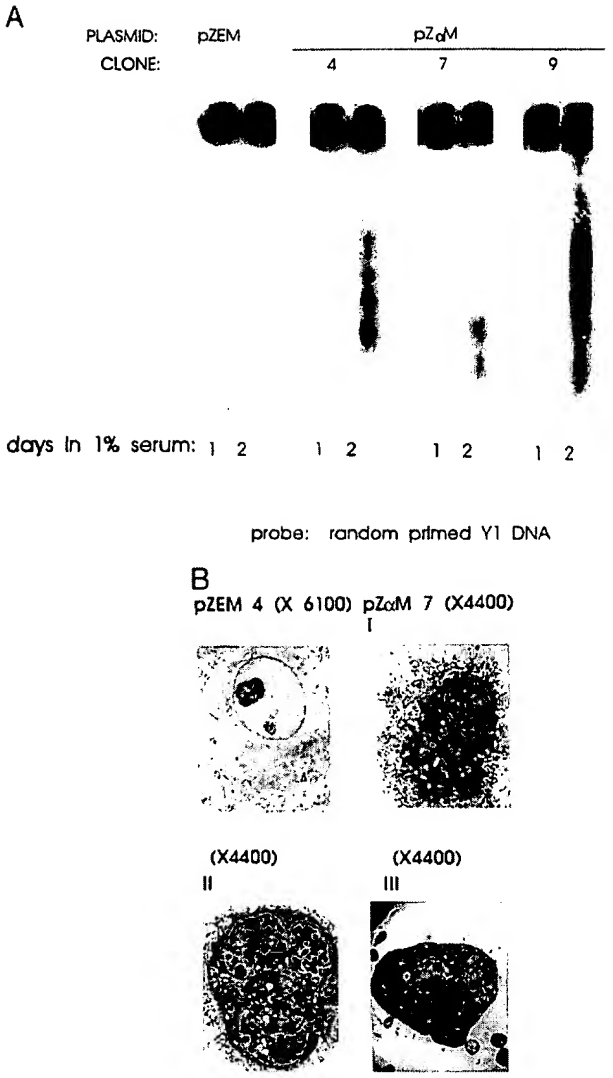

FIG. 5. **Survival and apoptosis of pZEM transfectants in serum-deprived medium.** *A*, the indicated transfectants were plated in 1% serum-containing medium and harvested after 1 and 2 days. Total cellular DNA was isolated, separated by agarose gel electrophoresis, transferred to nitrocellulose membrane, and probed with ^{32}P-labeled Y1 genomic DNA. A 180-bp internucleosomal ladder characteristic to cells dying via apoptosis can be seen in the pZαM transfectants only. *B*, Y1 transfectants were grown in 1% serum medium for 24 h, fixed, and analyzed by electron microscopy for early signs of apoptotic death; *I–III* are various sections (the magnification is indicated) of Y1 pZαM transfectants and pZEM control lines.

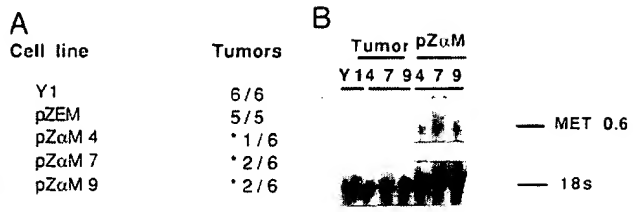

FIG. 6. ***In vivo* tumorigenicity of pZαM transfectants.** *A*, parental Y1 cells, a pZEM control line, and three pZαM transfectants (*4*, *7*, and *9*) were tested for their ability to form tumors in syngeneic LAF-1 mice. Tumor formation was assessed by palpation for 2 months after injection. The number of mice forming tumors is tabulated. The statistical significance of the difference between the control and antisense transfectants was determined using a test; $p > 0.001$. * indicates that these tumors were negative for pZαM expression. *B*, loss of antisense DNA MeTase expression in tumors derived from antisense transfectants. RNA (10 μg) isolated from the indicated tumors was subjected to Northern blot analysis and hybridization with the 0.6-kb MET cDNA probe. Expression of the 1.3-kb antisense message is seen only in the original cell lines pZαM (*4*, *7*, and *9*) and is undetectable in tumors arising from pZαM transfectants or Y1 cell lines even after long exposure. The filter was stripped of radioactivity and rehybridized with a ^{32}P-labeled oligonucleotide corresponding to 18 S rRNA (28).

of many nontumorigenic cells. As observation of the pZαM transfectants indicated that they expressed enhanced dependence on serum and limited survivability under serum-deprived conditions, we determined whether this limited survivability involved an enhancement or induction of an apoptotic program. While the control cells exhibited almost 100% viability up to 72 h after transfer into serum-deprived medium, all pZαM transfectants showed up to 75% loss of viability at 48 h.

To test whether the serum-deprived pZαM cells were dying as a result of an activated apoptotic death program, cells were plated in starvation medium and harvested at 24-h intervals, and total cellular DNA was isolated from the cells and analyzed by agarose gel electrophoresis. After 48 h in serum-starved conditions, pZαM transfectants exhibit the characteristic 180-bp internucleosomal DNA ladder while the control pZEM transfectants show no apoptosis at this time point (Fig. 5*A*).

To determine whether cells expressing antisense to the DNA MeTase exhibit early morphological markers of apoptosis, cells were serum-starved for 24 h, harvested, and analyzed by electron microscopy. Fig. 5*B* shows representative electron micrographs of several blocks of control pZEM and pZαM transfectants at various magnifications (*I–III*). The control cells have a fine uniform nuclear membrane whereas the pZαM cells exhibit the cardinal markers of apoptosis (34): condensation of chromatin and its margination at the nuclear periphery (*panels I* and *II*), chromatin condensation (*panel II*), nuclear fragmentation (*panel III*), formation of apoptotic bodies, and cellular fragmentation. Whereas it is still unclear whether apoptosis upon serum deprivation is directly enhanced by demethylation or is an indirect effect of the change in the transformed state of the transfectants, the serum deprivation-induced cell death is another indicator of the reversal of cellular transformation by DNA MeTase antisense.

To determine whether demethylation can result in inhibition of tumorigenesis *in vivo*, we injected 1×10^6 cells for each of the Y1, pZEM, and pZαM (4, 7, and 9) transfectants subcutaneously into the syngeneic mouse strain LAF-1. The presence of tumors was determined by palpation. While all the animals injected with Y1 or pZEM cells formed tumors, animals injected with the pZαM transfectants had very few tumors arise (Fig. 6*A*; $p > 0.005$).

One possible explanation for the fact that a small number of tumors did form in animals injected with the pZαM transfectants is that they are derived from revertants that lost expression of the antisense to the DNA MeTase under the selective pressure *in vivo*. RNA was isolated from tumors arising from the pZαM transfectants, and the level of expression of the 0.6-kb antisense message was compared with the transfectant lines *in vitro* (Fig. 6*B*). The expression of the antisense message is virtually nonexistent in the tumors derived from pZαM transfectants even after long exposure of the Northern blots, supporting the hypothesis that expression of an antisense message to the DNA MeTase is incompatible with tumor growth *in vivo*.

DNA Demethylation Induced by 5-AzaCdR Results in Reversal of Cellular Transformation ex Vivo—To further verify that inhibition of DNA methylation results in reversal of cellular transformation and to exclude the possibility that the effects observed are nonspecific results of antisense expression we used an inhibitor of DNA methylation 5-azadeoxycytidine (5-

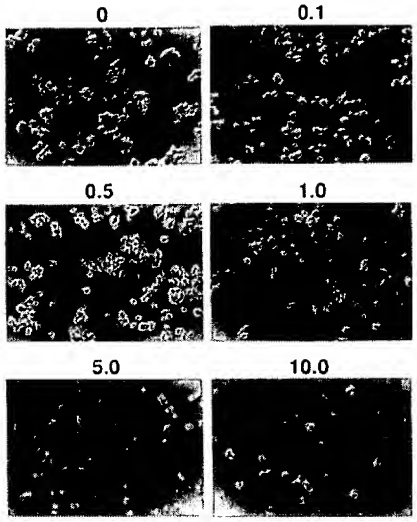

FIG. 7. **Morphological change in Y1 cells treated with 5-aza-CdR.** Y1 cells were treated with concentrations of 5-azaCdR ranging from 0–10 μM every 12 h for 72 h. Phase contrast microscopy at × 200 magnification of living cultures of the treated cells is presented.

azaCdR) that acts at a different site than antisense RNA (35). 5-azaCdR is a deoxycytidine analogue that inhibits DNA methylation once it is incorporated into DNA. It has been suggested that an irreversible complex is formed between the DNA MeTase enzyme and the C-6 position of the cytosine moiety (36). We treated Y1 cells with concentrations of 5-azaCdR ranging from 0 to 10 μM every 12 h for 72 h. 5-azaCdR increases the proportion of cytosine to methylcytosine in the DNA by 1.6-fold in a dose-dependent manner (0–5.0 μM) as determined by a nearest neighbor analysis. Over the same concentration range, cell viability in low serum is reduced from 80% to ~40%, and the ability of cells to form colonies in soft agar is reduced by ~50-fold. No differences were seen in the ability of cells to form colonies on regular plastic dishes. The 5-azaCdR-treated cells exhibited dose-dependent morphological changes similar to those observed in the pZαM transfectants (Fig. 7). This experiment suggests that 5-azaCdR treatment reversed the transformed phenotype of Y1 cells but did not affect their viability.

DISCUSSION

This paper tests the hypothesis that overexpression of the DNA MeTase plays a causal role in cellular transformation by expressing an antisense message to the DNA MeTase in an adrenocortical carcinoma cell line. Expression of an antisense DNA MeTase (Fig. 1) leads to: (i) a limited reduction in DNA MeTase steady state mRNA and protein levels (Fig. 2), (ii) a general but limited reduction in the methylation content of the genome (Fig. 2), (iii) demethylation of regions aberrantly methylated in this cell line such as the adrenal specific 21-hydroxylase gene (Fig. 3), (iv) morphological changes indicative of inhibition of the transformed phenotype, (v) inhibition of anchorage-independent growth as determined by soft agar assays, (vi) inhibition of serum-independent survivability and induction of apoptosis under serum-deprived conditions, as well as (vii) inhibition of tumorigenesis in syngeneic mice (Fig. 6) and (viii) inhibition of DNA methylation by 5-azaCdR, which acts at a site completely different from antisense to the DNA MeTase, also results in reversal of transformation indicators *ex vivo*. The fact that a 2-fold inhibition in DNA MeTase expression is sufficient to induce such profound changes in the state of transformation of Y1 cells is in accordance with previously published data showing that a 2–3-fold elevation in DNA MeTase activity by forced expression of an exogenous DNA MeTase in NIH 3T3 can induce cellular transformation of these cells (23). Whereas antisense expression is considered one of the most direct means to inhibit gene expression, no experimental method is devoid of potential complications. 5-azaCdR, which is the most commonly used DNA methylation inhibitor, has side effects (36, 37). However, the fact that both inhibitors had similar effects strongly validates our conclusions. The fact that 5-azaCdR inhibited transformation indicators but not the survival of the cells and their ability to form colonies, and the fact that the reversal of transformed phenotype was expressed weeks after the inhibitor had been removed is consistent with the model that 5-azaCdR triggered a change in the cellular program rather than a cytotoxic or cytostatic effect. It stands to reason that this change in program was triggered by the initial demethylation event caused by the drug.

Our experiments support a previously proposed hypothesis that overexpression of DNA MeTase is an important component of an oncogenic pathway(s) (22). Since Y1 is a line derived from a naturally occurring tumor (24) which bears amplified copies of Ras (25), it is possible that hyperactivation of the DNA MeTase is triggered by the Ras-Jun signaling pathway (21, 22). The DNA MeTase promoter bears a number of AP-1 sites (20), and we demonstrated that the activity of the DNA MeTase promoter is dependent on binding of AP-1 (21) and that down-regulation of the the Ras-Jun pathway in Y1 cells results in inhibition of DNA MeTase activity, hypomethylation, and reversal of the transformed phenotype.[2] Our data might explain previous observations demonstrating an increase in DNA MeTase activity (13, 19) in cancer cells by suggesting that this increase is critical for the transformed state.

What is the possible mechanism by which hypermethylation can cause cellular transformation? The answer to this question is still elusive and could not be resolved by the data presented in this paper; however, several hypotheses have been previously suggested. One plausible explanation that has been previously suggested by Baylin and his colleagues (38) is that methylation may establish abnormalities of chromatin organization which in turn mediate the progressive losses of gene expression associated with tumor development. One interesting class of genes that might be affected are the tumor suppressor genes. There is evidence that ectopic inactivation of tumor suppressor genes by methylation contributes to cancer (39, 40). The promoter region of the RB-1 gene was found to be methylated in 6 of 77 retinoblastomas (17), and the 5' region of the WT-1 gene was methylated in 2 out of 29 Wilms tumors (40), while the gene methylated was otherwise grossly normal. However, there is no evidence that tumor suppressor genes are the critical targets for hypermethylation in cancer cells or that tumor suppressor genes are selectively demethylated in the DNA MeTase antisense transfectants. Also, our unpublished data do not suggest any induction in the level of expression of these genes in the pZαM transfectants.

Another interesting mechanism that has been suggested by Jones and his colleagues is that methylated CpGs are hot spots for mutations by deamination of the methylated cytosine into thymidine (41). This kind of change induced by methylation will not be reversible, the fact that we could reverse transformation by inhibiting DNA MeTase suggests that other mechanisms must be involved. While inhibition of gene expression by methylation is the best analyzed function of DNA methylation, one should bear in mind that any function of the genome might be modified by methylation. Sites that are especially sensitive to changes in methylation might be controlling DNA functions such as repair, replication, and susceptibility to

[2] A. R. MacLeod, J. Roleau, and M. Szyf, unpublished results.

death program-related endonucleases.

One question that remains to be answered is how to explain the contradiction between the fact that DNA MeTase is overexpressed in cancer cells and the observed regional hypomethylation of the genome of many cancer cells (11, 12). However, there are no data at this stage to resolve this apparent contradiction. While additional experiments will be required to address these questions, this paper demonstrates that inhibition of DNA methylation leads to a reversal of the transformed state and that DNA methylation plays a critical role in cellular transformation.

Acknowledgments—We thank Dr. Gary Tanigawa, Marc Pinard, and Shyam Ramchandani for critical reading of the manuscript and stimulating discussions, as well as Vera Bozovic for excellent technical assistance, Allan Forester for help with the photography, and Marie Ballak for her contribution to the electron microscopy analysis.

REFERENCES

1. Razin, A., and Riggs, A. D. (1980) *Science* **210,** 604–610
2. Razin, A., and Szyf, M. (1984) *Biochim. Biophys. Acta* **782,** 331–342
3. Yisraeli, J., and Szyf, M. (1985) in *DNA Methylation: Biochemistry and Biological Significance* (Razin, A., Cedar, H., and Riggs, A. D., eds) pp. 353–378, Springer-Verlag, New York
4. Li, E., Bestor, T. H., and Jaenisch, R. (1992) *Cell* **69,** 915–926
5. Jones, P. A. (1985) *Cell* **40,** 485–486
6. Razin, A., Feldmesser, E., Kafri, T., and Szyf, M. (1985) in *Biochemistry and Biology of DNA Methylation* (Razin, A., and Cantoni, G. L., eds) p. 239, Alan R. Liss, Inc., New York
7. Szyf, M., Rouleau, J., Theberge, J., and Bozovic, V. (1992) *J. Biol. Chem.* **267,** 12831–12836
8. Szyf, M., Kaplan, F., Mann, V., Giloh, H., Kedar, E., and Razin, A. (1985) *J. Biol. Chem.* **260,** 8653–8656
9. Szyf, M., Bozovic, V., and Tanigawa, G. (1991) *J. Bol. Chem.* **266,** 10027–10030
10. Szyf, M. (1991) *Biochem. Cell Biol.* **64,** 764–769
11. Feinberg, A. P., Gehrke C. W., Kuo K. C., and Ehrlich, M. (1988) *Cancer Res.* **48,** 1159–1161
12. Feinberg, A. P., and Vogelstein, B. (1983) *Nature* **301,** 89–92
13. El-Deiry, W. S., Nelkin, B. D., Celano, P., Chiu-Yen, R. W., Falco, J. P., Hamilton, S. R., and Baylin, S. B. (1990) *Proc. Natl. Acad Sci. U. S. A.* **88,** 3470–3474
14. Antequera, F., Boyes, J., and Bird, A. (1990) *Cell* **62,** 503–514
15. de Bustros, A., Nelkin, B. D., Silverman, A., Ehrlich, G., Poiesz, B., and Baylin, S. B. (1988) *Proc. Natl. Acad Sci. U. S. A.* **85,** 5693–5697
16. Makos, M., Nelkin, B. D., Lerman, M. I., Latif, F., Zbar, B., and Baylin, S. B. (1992) *Proc. Natl. Acad Sci. U. S. A.* **89,** 1929–1933
17. Ohtani-Fujita, N., Fujita, T., Aoike, A., Osifchin, N. E., Robbins, P. D., and Sakai, T. (1993) *Oncogene* **8,** 1063–1067
18. Saxon, P. J., Srivatsan, E. S., and Stanbridge, E. G. (1986) *EMBO J.* **5,** 3461–3466
19. Kautiainen, T. L., and Jones, P. (1986) *J. Biol. Chem.* **261,** 1594–1598
20. Rouleau, J., Tanigawa, G., and Szyf, M. (1992) *J. Biol. Chem.* **267,** 7368–7377
21. Rouleau, J., MacLeod, A. R., and Szyf, M. (1995) *J. Biol. Chem.* **270,** 1595–1601
22. Szyf, M. (1994) *Trends Pharmacol. Sci.* **15,** 233–238
23. Wu, J., Issa, J. P., Herman, J., Bassett, D., Nelkin, B. D., and Baylin, S. B. (1993) *Proc. Natl. Acad. Sci. U. S. A.* **90,** 8891–8895
24. Yasumura, Y., Buonassisi, V., and Sato, G. (1966) *Cancer Res.* **26,** 529–535
25. Schwab, M., Alitalo, K., Varmus, H. E., Bishop, J. M., and George, D. (1983) *Nature* **303,** 497–501
26. Ausubel, F. M., Brent, R., Kingston, R. E., Moore, D. D., Smith, J. A., Seidman, J. G., and Struhl, K. (1988) *Current Protocols in Molecular Biology,* Wiley and Sons, New York
27. Freedman, V. H., and Shin, S. (1974) *Cell* **3,** 355–359
28. Bestor, T., Laudano, A., Mattaliano, R., and Ingram, V. (1988) *J. Mol. Biol.* **203,** 971–983
29. Szyf, M., Milstone, D. S., Schimmer, B. P., Parker, K. L., and Seidman, J. G. (1990) *Mol. Endocrinol.* **4,** 1144–1152
30. Maysinger, D., Piccardo, P., Flipovic-Grcic, J., and Cuello, A. C. (1993) *Neurochem Int.* **23,** 123–129
31. Szyf, M., Schimmer, B. P., and Seidman, J. G. (1989) *Proc. Natl. Acad. Sci. U. S. A.* **86,** 6853–6857
32. Jones, P. A., Wolkowicz, M. J., Rideout, W. M., III, Gonzales, F. A., Marziasz, C. M., Coetzee, G. A., and Tapscott, S. J. (1990) *Proc. Natl. Acad Sci. U. S. A.* **87,** 6117–6121
33. Barns, D., and Sato, G. (1980) *Cell* **22,** 649–655
34. Wyllie, A. H., Beatie, G. J., and Hargreaves, A. D. (1981) *Histochem. J.* **13,** 681–692
35. Wu, J. C., and Santi, D. V. (1985) *Biochemistry and Biology of DNA Methylation* (Razin, A., and Cantoni, G. L., eds) pp. 119–129, Alan R. Liss Inc., New York
36. Jones, P. A. (1984) in *DNA Methylation: Biochemistry and Biological Significance* (Razin, A., Cedar, H., and Riggs, A. D., eds) pp. 165–187, Springer-Verlag New York Inc., New York
37. Tammame, M., Antequera, F., Villanueva, J. R., and Santos, T. (1983) *Mol. Cell. Biol.* **3,** 2287–2297
38. Baylin, S. B., Makos, M., Wu, J., Chiu Yen, R.-W., de Bustros, A., Vertino, P., and Nelkin, B. D. (1991) *Cancer Cells* **3,** 383–390
39. Bestor, T. H., and Coxon, A.(1993) *Curr. Biol.* **3,** 384–386
40. Royer-Pokora, B., and Schneider, S. (1992) *Genes Chromosomes Cancer* **5,** 132–140
41. Jones, P. A., Rideout, W. M., Shen, J., Spruck, C. H., and Tsai, Y. C. (1992) *Bioessays* **14,** 33–36

EXHIBIT K

Proc. Natl. Acad. Sci. USA
Vol. 94, pp. 684–689, January 1997
Medical Sciences

Inhibition of tumorigenesis by a cytosine–DNA, methyltransferase, antisense oligodeoxynucleotide

SHYAM RAMCHANDANI*, A. ROBERT MACLEOD*, MARC PINARD*, ERIC VON HOFE†, AND MOSHE SZYF*‡

*Department of Pharmacology and Therapeutics, McGill University, Montreal, PQ, Canada H3G 1Y6; and †Hybridon, Inc., Worcester, MA 01605

Communicated by Robert L. Sinsheimer, University of California, Santa Barbara, CA, November 6, 1996 (received for review July 23, 1996)

ABSTRACT **This paper tests the hypothesis that cytosine DNA methyltransferase (DNA MeTase) is a candidate target for anticancer therapy. Several observations have suggested recently that hyperactivation of DNA MeTase plays a critical role in initiation and progression of cancer and that its up-regulation is a component of the Ras oncogenic signaling pathway. We show that a phosphorothioate-modified, antisense oligodeoxynucleotide directed against the DNA MeTase mRNA reduces the level of DNA MeTase mRNA, inhibits DNA MeTase activity, and inhibits anchorage independent growth of Y1 adrenocortical carcinoma cells *ex vivo* in a dose-dependent manner. Injection of DNA MeTase antisense oligodeoxynucleotides i.p. inhibits the growth of Y1 tumors in syngeneic LAF1 mice, reduces the level of DNA MeTase, and induces demethylation of the adrenocortical-specific gene C21 and its expression in tumors *in vivo*. These results support the hypothesis that an increase in DNA MeTase activity is critical for tumorigenesis and is reversible by pharmacological inhibition of DNA MeTase.**

Modification of DNA by methylation is now recognized as an important mechanism of epigenetic regulation of genomic functions (1–3). Methylation of DNA is a postreplication event catalyzed by the DNA methyltransferase (DNA MeTase) enzyme using *S*-adenosyl methionine as a methyl donor (4). Approximately 80% of cytosines located in the CpG dinucleotide sequence are methylated in the genome of most vertebrate cells, but the distribution of methylated sites is cell- and tissue-specific (5). Patterns of methylation are generated during development by enzymatic *de novo* methylation and demethylation processes (1–7) and are maintained in somatic cells.

A number of observations have suggested that the pattern of DNA methylation is disrupted in cancer cells (8, 9). Both hypomethylation (9) and hypermethylation (10–12) of different CpG sites in cancer cells and tissues relative to the cognate normal tissue have been documented. Some of the sites that are hypermethylated in tumors are located in tumor–suppressor loci such as p16 (13), retinoblastoma (14), von Hippel–Lindau (15), and Wilms tumor (16), and, recently, a new candidate tumor–suppressor gene was cloned by molecular analysis of the hypermethylated region in chromosome 17p13.3 (17). One possible explanation that has been proposed to explain the changes in DNA methylation observed in cancer cells is that they are the end result of a change in the enzymatic machinery controlling DNA methylation in the cell (7, 12, 18–20). In accordance with this hypothesis, cancer cell lines (21) and human tumors (22) have been shown to express elevated levels of DNA MeTase. Recently, Belinsky *et al.* (23) showed that increased DNA MeTase activity is an early event in carcinogen-initiated lung cancer in the mouse. Forced expression of DNA MeTase cDNA in murine NIH 3T3 cells leads to genomic hypermethylation and neoplastic transformation (24), and expression of an antisense mRNA to the DNA MeTase leads to loss of tumorigenicity of the adrenocortical carcinoma cell line Y1 (25).

Many stimuli may account for increased DNA MeTase activity in tumors. One possible molecular mechanism explanation of this elevation of DNA MeTase in cancer cells is that the expression of the DNA MeTase gene is regulated by oncogenic signaling pathways such as the Ras–Jun signaling pathway (18, 19). Modulation of this pathway can alter DNA MeTase expression and DNA methylation (26–28). Similarly, ectopic expression of *Ha–ras* leads to induction of demethylation activity in P19 cells (29), which can explain (18) the observed hypomethylation of some CpG sites in cancer cells (8, 9).

If hyperactivity of DNA MeTase is a critical, downstream component of oncogenic programs (25–28), it should be an excellent target for anticancer therapy (19). To test this hypothesis in an animal model, specific inhibitors of DNA MeTase are required. The only DNA MeTase inhibitor that has been available to date is the nucleoside analog 5-azadeoxycytidine (30). Although 5-azadeoxycytidine is an effective inhibitor of DNA methylation (30), it has many side effects that might compromise the interpretation of the experimental data and limit its clinical utility (19, 31, 32). The advent of antisense oligodeoxynucleotides as specific inhibitors of protein expression in whole animal systems offers new opportunities in approaching this hypothesis (33).

Y1 cells offer a model to test our hypothesis. First, this line [which was isolated from a naturally occurring adrenocortical tumor in an LAF1 mouse (34)] bears a 30- to 60-fold amplification of the cellular proto oncogene c-Ki-*ras* (35). Second, the molecular link between hyperactivation of Ras, DNA MeTase hyperactivity, and DNA methylation and the state of cellular transformation has been recently demonstrated (25, 28). Third, identification of effective antisense oligodeoxynucleotide inhibitors requires screening of a number of potential candidates. This can only be done effectively *ex vivo*. Y1 cells can be grown and tested for tumorigenic characteristics *ex vivo* as well as implanted in syngeneic LAF1 mice (25) *in vivo*, thus enabling the study of the effects of inhibition of DNA methylation in a whole animal system.

MATERIALS AND METHODS

Cell Culture, *ex Vivo* Oligodeoxynucleotide Treatment, and Tumorigenicity Assays. Y1 cells were maintained as monolayers in F-10 medium, which was supplemented with 7.25% heat-inactivated horse serum and 2.5% heat-inactivated fetal calf serum (Immunocorp, Montreal). The sequences of the oligodeoxynucleotides used in this study were as follows: antisense (HYB101584), 5′-TCT ATT TGA GTC TGC CAT TT-3′ corresponding to bases −2 to +18 in the murine DNA MeTase mRNA [relative to the putative translation initiation site (9)]; the scrambled sequence corresponding to the antisense sequence (HYB102277), 5′-TGT GAT TCT CCT TAT

The publication costs of this article were defrayed in part by page charge payment. This article must therefore be hereby marked "*advertisement*" in accordance with 18 U.S.C. §1734 solely to indicate this fact.

0027-8424/97/94684-6$2.00/0
PNAS is available online at http://www.pnas.org.

Abbreviation: DNA MeTase, DNA methyltransferase.

‡To whom reprint requests should be addressed.

TCG AT-3′; and the reverse sequence (HYB101585), 5′-TTT ACC GTC TGA GTT TAT CT-3′. Phosphorothioate oligodeoxynucleotides were synthesized using phosphoramadite chemistry on a Biosearch model 8700 automated synthesizer and were purified by HPLC using a phenyl Sepharose column followed by DEAE 5PW anion exchange chromatography. The purity of all oligonucleotides was greater than 98% as determined by ion exchange chromatography. These experiments were performed in the absence of any lipid carrier to avoid nonspecific effects of the carrier in long term treatments and to recapitulate the situation *in vivo*, in which no carrier was used. This experimental paradigm required using oligodeoxynucleotides at the micromolar concentration range, which is higher than the concentrations required when lipid carriers are used.

DNA and RNA Analyses. Genomic DNA was prepared from pelleted nuclei, and total cellular RNA was prepared from cytosolic fractions according to standard protocols (36–38).

Western Blot Analysis of DNA MeTase. Rabbit polyclonal antibodies were raised (Pocono Rabbit Farm, Canadensis, PA) against a peptide sequence consisting of amino acids 1107–1125 of the mouse DNA MeTase (1101–1119 of the human DNA MeTase). The specificity of the polyclonal serum was tested by competition with the antigen peptide. Nuclear extracts (50 μg) were resolved on a 5% SDS/PAGE, transferred onto poly(vinylidene difluoride) membrane (Amersham), and subjected to immunodetection for the DNA MeTase according to standard protocols using a 1:2000 dilution of primary antibody and an enhanced chemiluminescence detection kit (Amersham) (40).

Assay of DNA MeTase Activity. DNA MeTase activity (3 μg) was assayed by incubating 3 μg of nuclear extract with a synthetic, hemimethylated, double-stranded oligodeoxynucleotide (37) substrate and *S*-[*methyl*-^{3}H]-*S*-adenosyl-L-methionine (78.9 Ci/mmol; Amersham) as a methyl donor for 3 h at 37°C as described (36).

Assay of C21 mRNA by Reverse Transcriptase–PCR. The expression of the C21 gene was determined using our described primers and amplification conditions (41).

RESULTS

Antisense Oligodeoxynucleotides to the Translation Initiation Region of the Murine DNA MeTase Inhibit DNA MeTase mRNA, DNA MeTase Activity, and Tumorigenesis *ex Vivo*. We have shown that expression of a 600-bp fragment bearing sequences encoding the 5′ domain of the DNA MeTase mRNA in

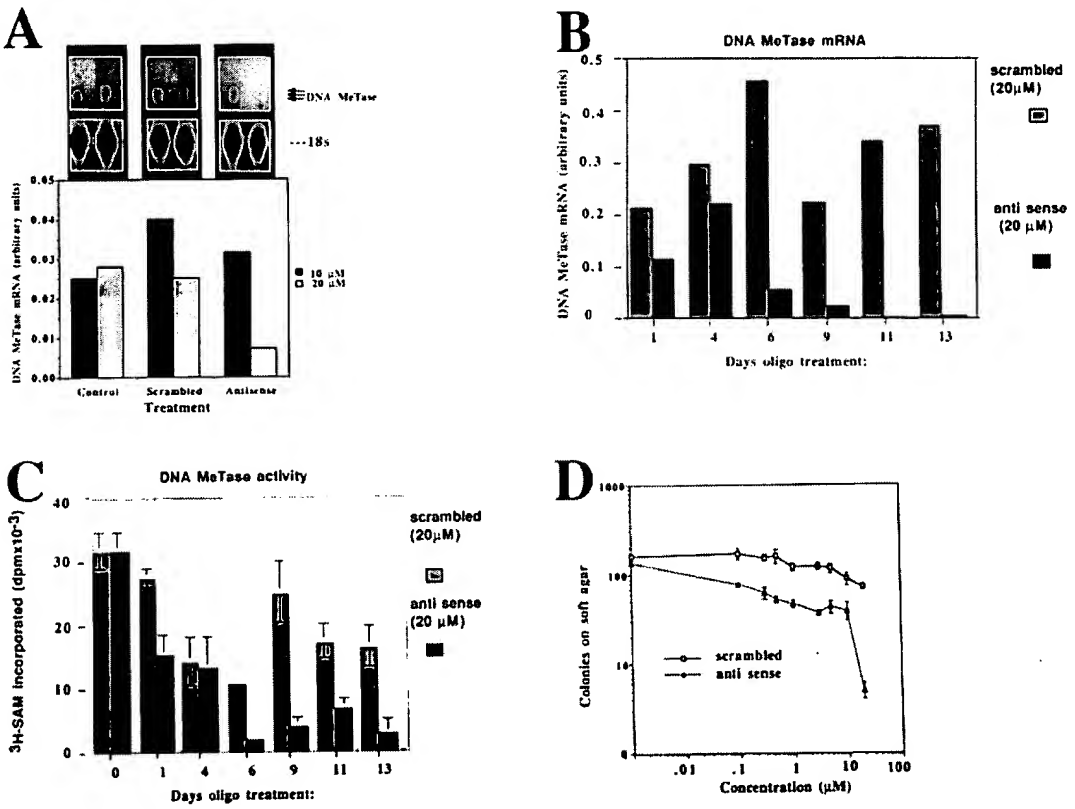

FIG. 1. DNA MeTase antisense oligodeoxynucleotides inhibit DNA MeTase mRNA, DNA MeTase activity, and anchorage independent growth *ex vivo*. (*A*) RNase protection analysis of DNA MeTase mRNA in Y1 cells treated with control scrambled and antisense oligodeoxynucleotides. Y1 cells were cultured in the presence of different concentrations of scrambled and antisense oligodeoxynucleotides (sequence shown in *Materials and Methods*) as indicated for 48 h. RNA (3 μg) extracted from the cells was subjected to an RNase protection assay as described (26) using a 700-bp riboprobe [probe A in Rouleau *et al.* (26)] encoding the DNA MeTase genomic sequence from −0.39 to +318. The major bands representing the two major initiation sites are indicated (92-, 90-bp, protected fragments) as well as the first exon, which gives a 99-bp, protected fragment. (*B*) Time course of inhibition of DNA MeTase mRNA by antisense oligodeoxynucleotides. Y1 cells were incubated in the presence of 20 μM of either antisense or scrambled oligodeoxynucleotides, and the medium was replaced with oligodeoxynucleotide-containing medium every 24 h. Cells were harvested at the indicated time points, and RNA and nuclear extracts were prepared as described. RNA was subjected to RNase protection assay as described in *A*. An autoradiogram similar to the one presented in *A* was scanned, and the amount of DNA MeTase mRNA at each point was normalized to the signal obtained for 18s ribosomal RNA. (*C*) Nuclear extracts prepared from oligodeoxynucleotide-treated Y1 cells described in *B* were assayed for DNA MeTase activity as described. The results represent an average of triplicate determination ± SD. (*D*) Y1 cells were treated with scrambled and antisense oligodeoxynucleotides as described in *B* and seeded onto soft agar for determination of anchorage-independent growth as described. The results represent an average of triplicate determinations ± SD.

the antisense orientation can inhibit DNA methylation and induce both cellular differentiation of 10T½ cells (43) and reversal of transformation of Y1 cells (25). Antisense expression vectors could not be used easily to study the function and therapeutic potential of inhibiting DNA MeTase *in vivo*. We therefore tested the possibility that shorter antisense oligodeoxynucleotides directed against the same region of the mRNA could recapitulate these effects. An antisense oligodeoxynucleotide [+18 to −2 (sequence as in *Materials and Methods*) when the translation initiation site is indicated, as in Bestor *et al.* (44)] was found to be active in a preliminary screen, and we further determined its mechanism of action.

One of the possible mechanisms of action of antisense oligodeoxynucleotides is targeting RNase H activity to the RNA–DNA duplex, resulting in degradation of the mRNA (45). We first determined the dose–response relationship of

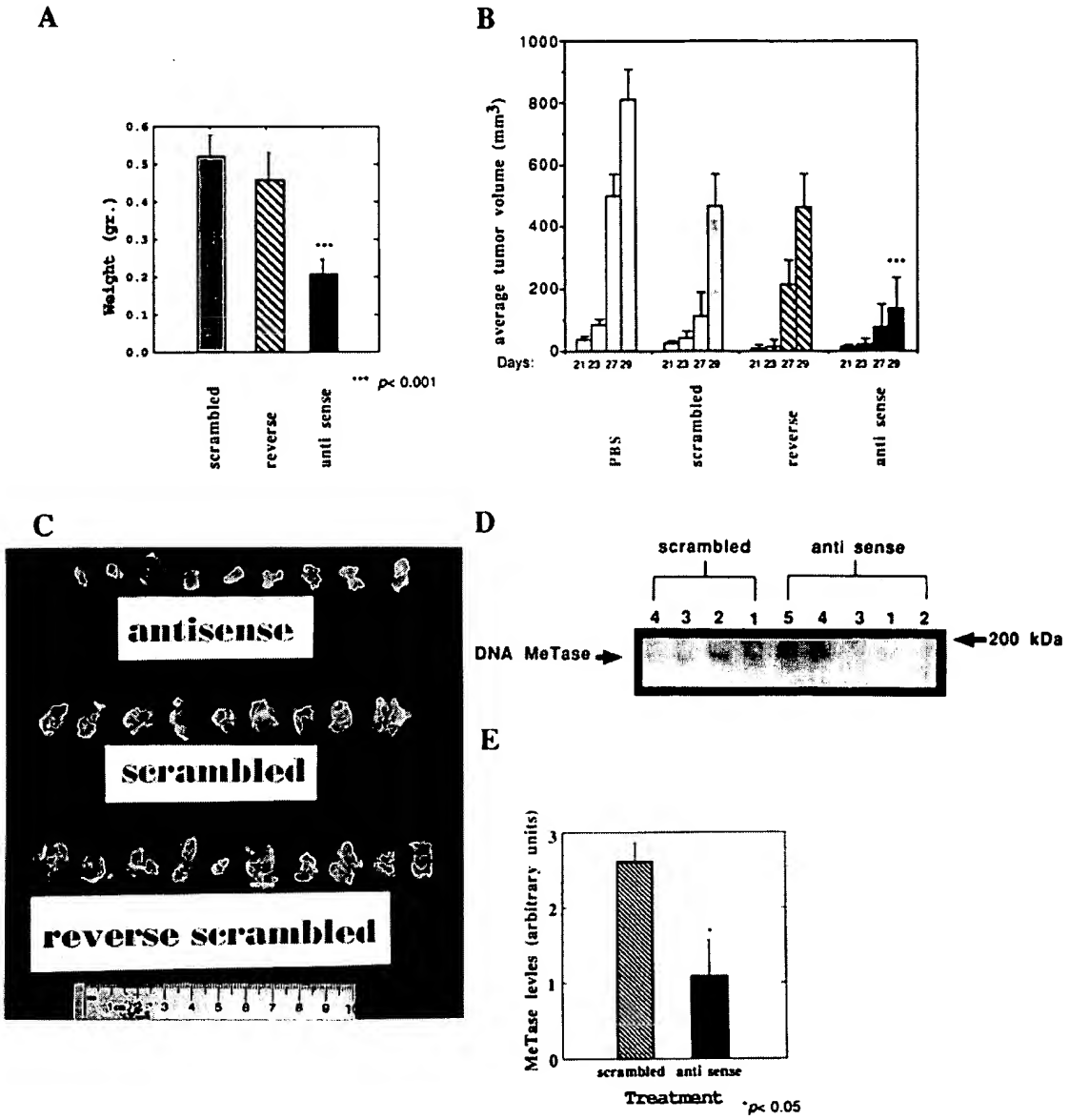

FIG. 2. DNA MeTase antisense oligodeoxynucleotide inhibits tumor growth *in vivo*. (*A*) Average weight of tumors isolated from LAF1 mice bearing Y1 tumors that were injected with antisense, scrambled, or reverse oligodeoxynucleotide (5 mg/kg) every 48 h for 29 days. The results are presented as an average ± SEM. The statistical significance of the difference between the scrambled or reverse groups and the antisense group was determined by a Student's *t* test to be $P < 0.001$. There was no statistically significant difference between the two control groups ($P > 0.5$). (*B*) Average volume of tumors determined as described at the indicated time points postimplantation [determined as described in Plumb *et al.* (42)]. (*C*) Photograph of the tumors removed from the antisense, reverse, and scrambled oligodeoxynucleotide-treated mice described above. (*D*) LAF1 mice bearing Y1 tumors were injected with 5 mg/kg scrambled ($n = 4$) or antisense ($n = 5$) oligodeoxynucleotides three times every 24 h s.c. Tumors were removed from each mouse (indicated by serial numbers 1–4 for the scrambled group and 1–5 for the antisense group), and nuclear extracts prepared from the tumors were subjected to a Western blot analysis as described. The band corresponding to the DNA MeTase is indicated by an arrow. The amount of signal corresponding to the DNA MeTase (OD arbitrary units) was normalized to the level of total protein transferred onto the membrane as determined by Amido black staining and quantified by scanning (OD arbitrary units). The values obtained (OD of DNA MeTase signal divided by OD of the total protein staining) for the tumors extracted from each of the treated mice (serial number of mice in bold) were as follows: scrambled: 1, 2.2; 2, 3.1; 3, 2.7; and 4, 2.5: antisense: 1, 0.6; 2, 0.5; 3, 0.16; 4, 1.0; and 5, 2.9. (*E*) Average DNA MeTase level per group is plotted with the SEM. The difference between the scrambled and antisense groups was determined by a Student's *t* test to be statistically significant ($P < 0.05$).

DNA MeTase mRNA abundance and DNA MeTase antisense oligodeoxynucleotide concentration at one time point. Y1 cells (10^6 cells) were treated with different concentrations (0, 10, and 20 μM) of antisense oligodeoxynucleotides and scrambled controls for 48 h. Cellular RNA was subjected to an RNase protection assay as described in *Materials and Methods*. The results presented in Fig. 1*A* demonstrate a sharp decrease in abundance of DNA MeTase mRNA after incubation of the cells with 20 μM of the DNA MeTase antisense oligodeoxynucleotides, which was not observed after treatment with scrambled oligodeoxynucleotides. We then defined the time dependence of reduction in DNA MeTase activity at the inhibitory concentration of the antisense oligodeoxynucleotide (20 μM). The results presented in Fig. 1 *B* (RNA) and *C* (MeTase activity) show that both DNA MeTase activity and mRNA are reduced by 10- to 100-fold after 6 days of treatment. Some fluctuations are observed in the levels of DNA MeTase in Y1 cells treated with control oligodeoxynucleotides (2-fold) as well as antisense oligodeoxynucleotides (such as the relatively high levels of DNA MeTase at 4 days). These oscillations in DNA MeTase mRNA expression might reflect changes in the cell cycle kinetics of the cells at different time points because DNA MeTase levels are regulated with the cell cycle (35, 37). Alternatively, they might result from nonspecific effects of oligodeoxynucleotides on different cellular parameters or reflect some inaccuracies in our measurements. However, an overall reduction in DNA MeTase activity was established after 6 to 9 days of treatment with the antisense oligodeoxynucleotides.

Can DNA MeTase antisense oligodeoxynucleotides induce a dose-dependent inhibition of tumorigenicity *ex vivo* as measured by anchorage-independent growth on soft agar? Y1 cells were treated with a range of concentrations of antisense and scrambled oligodeoxynucleotides (0–20 μM) for 13 days. The cells were harvested and plated onto soft agar as described (39). The results presented in Fig. 1*D* demonstrate a dose-dependent inhibition of colony formation on soft agar in antisense-treated cells vs. the scrambled control. The drop in the number of colonies formed on soft agar between 10 and 20 μM corresponds to the precipitous drop in DNA MeTase mRNA at this concentration of antisense oligodeoxynucleotide (Fig. 1*A*).

Inhibition of anchorage-independent growth of antisense-treated cells was observed even though the soft agar medium was not supplemented with antisense oligodeoxynucleotides, suggesting that the changes in the level of tumorigenicity of antisense-treated cells were irreversible. This is consistent with the hypothesis that, once DNA MeTase is inhibited, the cells are reprogrammed to a less transformed state (18, 25). The experiments described above demonstrated that antisense oligodeoxynucleotides could inhibit DNA MeTase activity *ex vivo* and that this inhibition corresponded to a dose-dependent inhibition of tumorigenicity.

Inhibition of Tumor Growth and DNA MeTase *in Vivo* by a DNA MeTase Antisense Oligodeoxynucleotide. To test the hypothesis that inhibition of DNA MeTase *in vivo* can result in inhibition of tumor growth and to determine the general toxic effects of DNA MeTase antisense treatment, Y1 cells (1×10^6) were implanted in the flank of the syngeneic mouse strain LAF1 and were treated by i.p. injections every 48 h with PBS, antisense oligodeoxynucleotide, or two control oligodeoxynucleotides: a scrambled version of the antisense oligodeoxynucleotide and a reverse sequence (see *Materials and Methods* for sequence). Preliminary experiments with a small number of animals per group ($n = 3$) established a dose-dependent relationship between oligodeoxynucleotide concentrations and tumor growth. No effects were observed at 0.5 mg/kg whereas inhibition of tumor appearance and growth was observed in the 1- to 5-mg/kg range. At 20 mg/kg, nonspecific effects were observed with the scrambled oligodeoxynucleotides in two out of three experiments whereas a statistically significant reduction in tumor growth with antisense oligodeoxynucleotides vs. controls was observed in one experiment (data not shown). Forty LAF1 mice were implanted with Y1 cells, randomized, and divided into color-coded groups of 10 mice each and were treated and evaluated as follows in a double-blind fashion. Three days postimplantation, the mice were injected i.p. with 100 μl of PBS or PBS containing 5 mg/kg of either antisense, scrambled, or reverse oligodeoxynucleotides. Injections were repeated every 48 h, and tumor diameter measurements were taken at each time point. Thirty days postinjection, the animals were killed, and tumors were excised and weighed. The results described in Fig. 2 show that tumor growth was inhibited by injection of DNA MeTase antisense oligodeoxynucleotides relative to control oligodeoxynucleotides as determined by the rate of increase in the average tumor volume (Fig. 2*B*) as well as by the final weight and size of the tumors (Fig. 2 *A* and *C*). The difference in the average tumor volume between the antisense-treated group and either of the different control groups (PBS, scrambled, and reverse) at 29 days was highly statistically significant, as determined by a Student's t test ($P < 0.005$) whereas the difference between the different control oligodeoxynucleotide-treated groups and the PBS-treated group was not statistically significant. Similarly, the difference in average final tumor weight at 30 days between the antisense- and control oligodeoxynucleotide-treated groups was highly statistically significant ($P < 0.001$). One of the antisense-treated animals did not develop tumors whereas all of the members of the control groups developed tumors (one mouse of the reverse group died with a heavy tumor load before termination of the experiment).

We determined the general toxic effects of *in vivo* DNA MeTase antisense oligodeoxynucleotide treatment vs. treatment with the control oligodeoxynucleotides. Blood parameters and weight loss of antisense-, reverse-, and scrambled-injected (20 mg/kg) tumor-bearing LAF1 mice ($n = 5$) were assayed. As shown in Table 1, there were no significant reductions in red blood cell count, hematocrit, or percentage of hemoglobin in DNA MeTase antisense-treated animals vs. controls. Similarly, platelet and white blood cell counts were not increased but rather were decreased slightly in antisense-treated animals (Table 1). There was no significant weight loss even though tumor load was decreased significantly in this experiment by DNA MeTase antisense oligodeoxynucleotides.

These experiments demonstrated that *in vivo* treatment of tumor-bearing LAF1 mice with DNA MeTase antisense oligodeoxynucleotides can inhibit tumor growth, supporting the hypothesis that DNA MeTase is a critical component in maintaining the transformed state and that *in vivo* treatment with an antisense-based inhibitor of DNA MeTase can inhibit tumor growth.

DNA MeTase Antisense Oligodeoxynucleotide Inhibits DNA MeTase Levels, Induces Limited Demethylation of the

Table 1. Hematological analysis of LAF1 mice treated with antisense or control oligodeoxynucleotides (20 mg/kg) for 30 days ($n = 5$).

Treatment	Hematocrit	% hemoglobin	WBC	RBC	Platelets
Reverse	17.2 ± 9.2	6.4 ± 3.3	59.6 ± 2.19	3.4 ± 2.19	514 ± 291
Scrambled	16.1 ± 2.5	6.16 ± 0.9	71.8 ± 21.9	2.99 ± .45	503.2 ± 104
Antisense	21.9 ± 9.5	7.44 ± 3.8	50.7 ± 33	4.4 ± 1.8	302 ± 95

WBC, RBC, and hematocrit in g/dcl. Numbers represent mean and SD.

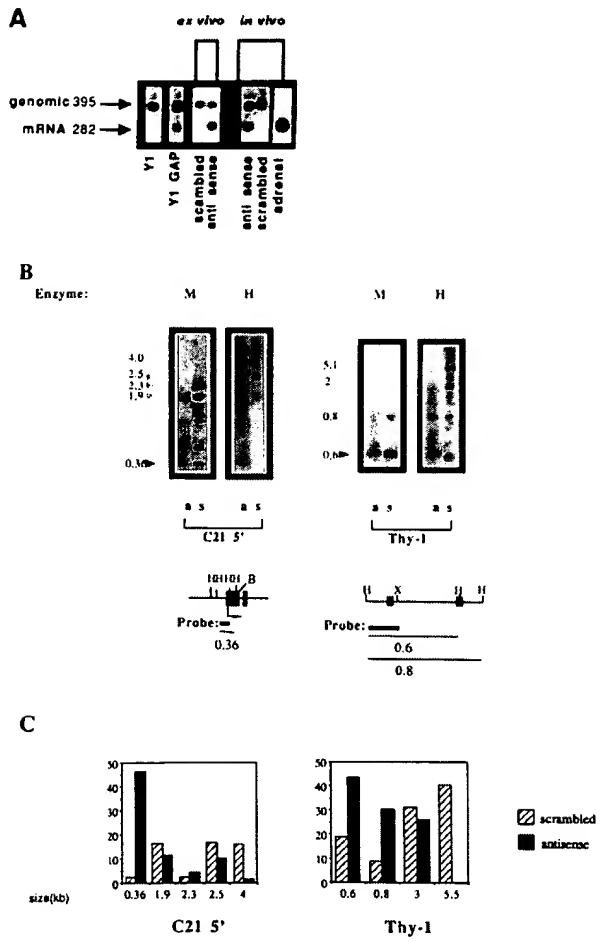

FIG. 3. Expression and demethylation of the C21 gene in Y1 tumors isolated from LAF1 mice treated with antisense oligodeoxynucleotides. (*A*) C21 expression was determined by reverse transcriptase–PCR amplification with C21-specific primers of total RNA isolated from Y1 cells, Y1GAP transfectants expressing hGAP (a GTPase- activating protein), an attenuator of Ras activity (28), Y1 cells treated with 20 μM of either scrambled oligodeoxynucleotide or DNA MeTase antisense oligodeoxynucleotides (*ex vivo* as indicated), Y1 tumors from LAF1 mice injected with either 5 mg/kg of scrambled or DNA MeTase antisense oligodeoxynucleotides (*in vivo*) as well as adrenal RNA. C21 plasmid DNA encoding the C21 gene (46) was included in the amplification reaction to control for nonspecific inhibition of amplification. The expected genomic and C21 mRNA amplification products are indicated by arrows. (*B*) DNA was extracted from Y1 tumors isolated from LAF1 mice injected with either scrambled oligodeoxynucleotides (scrambled 4, indicated as s) or antisense oligodeoxynucleotides (antisense 3, indicated as a) for 3 days as described. The DNA was subjected to *Hin*dIII digestion followed by either *Hpa*II (*H*) (which cleaves the sequence CCGG when the internal C is not3 methylated) or *Msp*I (*M*) (which cleaves the sequence CCGG even when the internal C is methylated) agarose gel fractionation (2.5%), Southern blotting analysis, and hybridization with the indicated probes. For the promoter region of the C21 gene, complete digestion of the gene should result in a 0.36-kb fragment (46), as indicated by the dark arrow. The partially methylated fragments are indicated by shaded arrows. The partial cleavage with *Msp*I is a consequence of the fact that the *Msp*I sites are nested within a *Hae*III site. These sites are highly resistant to cleavage by *Msp*I when fully or partially methylated, as described (47). For Thy-1, DNA prepared from the tumors indicated was subjected to a similar *Hpa*II–*Msp*I restriction enzyme analysis and hybridization with a 0.36 probe from the 5′ region of the *thy-1* gene (48). The expected *Hpa*II fragment is indicated by a dark arrow. Partially methylated fragments are indicated by shaded arrows. (*Lower*) Physical maps of the sequences analyzed for their methylation state. The first exons of the three genes are shown and are indicated as filled boxes, the probes used are indicated as thick lines, and the thin line indicates the expected nonmethylated and partially methylated *Hpa*II fragments. (X, *Xba*I; B, *Bam*HI). (*C*) Relative abundance of the *Hpa*II fragments was determined by densitometry as described. The size in kilobases of the scanned fragments is indicated. The results are presented as intensity of a specific fragment as a percentage of the total intensity in all scanned fragments per lane.

Adrenocortical-Specific C21 Gene, and Reactivates It. To determine whether injection of DNA MeTase antisense oligodeoxynucleotide can inhibit DNA MeTase activity, we treated tumor-bearing LAF1 mice for 3 days with either DNA MeTase antisense oligodeoxynucleotide (n = 5; 5 mg/kg) or the scrambled oligodeoxynucleotide (n = 4; 5 mg/kg) by s.c. injection near the tumor (1 cm) for 3 days. To limit (as much as possible) complicating, indirect factors that might have clouded the interpretation of data, we did not look at DNA methylation in tumors that were chronically treated. Tumors were harvested, nuclear extracts were prepared, and DNA MeTase levels in the nuclear extracts were determined by a Western blot analysis as described. The results of such an analysis are demonstrated in Fig. 2*D*, and the normalized average levels of DNA MeTase in each of the treatment groups plotted in Fig. 2*E* demonstrate a statistically significant reduction in DNA MeTase levels in antisense-treated animals ($P < 0.05$). The level of inhibition varied, however, from 90% inhibition in mouse number 3 in the group treated with antisense (Fig. 2*D*, lane 3) to no detectable inhibition in mouse number 5 (Fig. 2*D*, lane 5).

C21 is specifically expressed in the adrenal cortex, and the enzyme encoded by this gene, steroid 21 hydroxylase, is required for the synthesis of glucocorticoids, which is the main normal function of this tissue. The gene is expressed at very high levels in the adrenal cortex but is totally repressed and heavily methylated in Y1 tumor cells (41). No C21 mRNA is detected in Y1 cells even when the most sensitive assays, such as reverse transcriptase–PCR, are used (41). We have not observed any expression of C21 in Y1 cells in multiple Y1 cultures in the last decade under any conditions. We have suggested that this is a consequence of the increase in *de novo* DNA methylation activity in these cancer cells (41). Reexpression of C21 could serve as a good marker of demethylation and the reprogramming of Y1 cells to a nontransformed state.

To address this question, we performed a reverse transcriptase–PCR analysis of C21 expression on RNA prepared from the following samples: Y1 cells treated with either antisense DNA MeTase or scrambled oligodeoxynucleotides (20 μM) *ex vivo*; a tumor isolated from a mouse treated with antisense oligodeoxynucleotides *in vivo* for 3 days (antisense 3 exhibited the highest reduction in DNA MeTase activity: 90%); and Y1 cells transfected with hGAP [which attenuates the Ras signaling pathway, resulting in inhibition of DNA MeTase activity and partial demethylation of the C21 gene (28)]. C21 expression was induced under all of these conditions (Fig. 3*A*). This is the first induction of C21 reexpression in Y1 cells under any conditions observed in our laboratory. These results strongly support the hypothesis that DNA MeTase antisense oligodeoxynucleotides induce a partial demethylation and reprogramming of gene expression in Y1 cells that is similar to that observed after attenuation of the Ras signaling pathway.

To determine whether the 5′ promoter region of the C21 gene was demethylated in tumor DNA after antisense treatment, tumor DNA was subjected to *Msp*I/*Hpa*II restriction enzyme analysis, Southern blotting, and hybridization with a 5′ C21 probe [0.36-kb *Xba*I–*Bam*HI fragment encoding the promoter region of the C21 gene (41)]. Hypomethylation of the two *Hpa*II sites in the promoter region will result in a 0.36-kb fragment. As shown in Fig. 3*B*, the Y1 tumor that was extracted from a mouse (antisense 3) that was injected with antisense

oligodeoxynucleotides *in vivo* exhibits an increase in the abundance (as determined by densitometric analysis; Fig. 3*C*) of the 0.36-kb *Hpa*II fragment relative to the partially methylated fragments at 1.9, 2.5, and 4 kb compared with the control tumor. Demethylation of C21 is observed in other tumors injected with antisense (data not shown).

CpG island-containing genes are *de novo* methylated in tumor cells (13, 49–51). We therefore determined the state of methylation of a generally expressed CpG island-containing gene, *thy-1*, in mice treated with either antisense or control oligodeoxynucleotides. There was an increase in the relative abundance of the 600-bp *Hpa*II fragment contained in the 5′ *thy*-1 CpG island (48) (Fig. 3*B*) and a decrease in the relative abundance of the partial *Hpa*II fragments (≈3–5.5 kb) in tumors extracted from antisense-treated mice (labeled "a" in Fig. 3*B*) relative to the pattern observed in the control tumor (labeled "s" in Fig. 3*B*) (see Fig. 3*C* for quantification). These experiments demonstrated limited hypomethylation in tumor DNA in response to DNA MeTase antisense treatment *in vivo*.

DISCUSSION

The goal of this study was to test the hypothesis that tumorigenesis could be reversed by pharmacological inhibition of DNA MeTase activity and to suggest that DNA MeTase inhibitors could serve as potential anticancer agents. This study demonstrated that an antisense oligodeoxynucleotide directed against DNA MeTase mRNA can inhibit, in a dose-dependent manner, DNA MeTase mRNA expression, DNA MeTase activity, and tumorigenesis *ex vivo* and *in vivo*. Similar effects were not observed when a scrambled sequence was used. This is consistent with the hypothesis that the observed effects are a result of reduction in the level of DNA MeTase. The sequences used in our experiments did not bear the CG sites or G quartets that have been shown to bear nonantisense-related immunogenic and antitelomerase effects (52, 53). Although it is clear that phosphorothioate oligodeoxynucleotides might exhibit nonspecific antitumorigenic effects, our experiments revealed that the nonspecific and sequence-specific effects could be differentiated. One interesting question that was not addressed by this experiment is whether there is a critical size or level of tumor organization that is not treatable by DNA MeTase antisense inhibitors. Future studies will directly address this question.

Why are elevated levels of DNA MeTase critical for maintaining the cancer state? Three models have been suggested. (*i*) Elevated levels of DNA MeTase might result in disruption of the appropriate gene expression profile of a cell, leading to inactivation of tumor suppressor genes (17) and other genes that are characteristic of the differentiated state of the cell, such as C21 in Y1 cells (41). (*ii*) High levels of DNA MeTase might have a direct effect on origins of replication (18, 19). (*iii*) Methylated cytosines are hot spots for mutation, and deamination of methylated cytosines will result in C-T transition mutations (54).

Although more data are required to determine which of these mechanisms is involved in the genesis and maintenance of cancer, two issues are critical for the pharmacological and therapeutic application of DNA MeTase inhibitors. First, are the changes caused by aberrant methylation in carcinogenesis irreversible, as has been suggested (55), or are they reversible by pharmacological intervention? *Min* mice bearing a mutation in the homolog of the human repair-associated tumor suppressor gene *APC* were protected from formation of adenopolyps in the intestines when treated prophylactically with 5-azadeoxycytidine early after birth (55). The development of polyps could not be reversed when 5-azadeoxycytidine was applied later, suggesting an irreversible mechanism.

Second, is the aberrant methylation observed in cancer a consequence of the enhanced levels of DNA MeTase and therefore reversible by reducing the level of DNA MeTase (18, 19)? Although additional experiments will be required to demonstrate that similar results to those reported here can be obtained with cancers formed in the animal rather than in implanted tumors, our results lend support to the hypothesis that the effects of DNA MeTase induction are reversible and therefore suggest that DNA MeTase be a target for anticancer intervention.

We thank Dr. Kirk Field for critical reading of the manuscript and his thoughtful suggestions. We also thank Deanna Collier, Vera Bozovic, and Johanne Theberge for excellent technical assistance. This research was supported by the National Cancer Institute Canada, by a contract with Hybridon, Inc. (Worcester, MA), and by MethylGene, Inc. (Montreal).

1. Razin, A. & Riggs A. D. (1980) *Science* **210**, 604–610.
2. Razin, A. & Cedar, H. (1991) *Microbiol. Rev.* **55**, 451–458.
3. Tate, P. H. & Bird, A. P. (1993) *Curr. Opin. Genet. Dev.* **3**, 226–231.
4. Adams, R. L., McKay, E. L., Craig, L. M. & Burdon, R. H. (1979) *Biochim. Biophy. Acta* **561**, 345–57.
5. Yisraeli, J. & Szyf, M. (1984) in *DNA Methylation and Its Biological Significance*, eds. Razin, A. Cedar, H. & Riggs, A. D. (Springer, New York), pp. 353–378.
6. Razin, A. & Kafri, T. (1994) *Prog. Nucleic Acid Res. Mol. Biol.* **48**, 53–81.
7. Szyf, M. (1991) *Biochem. Cell Biol.* **69**, 764–767.
8. Gama-Sosa, M. A., Midgett, R. M., Slagel, V. A., Githens, S., Kuo, K. C., Gehrke, C. W. & Ehrlich, M. (1983) *Biochim. Biophys. Acta* **740**, 212–219.
9. Feinberg, A. P. & Vogelstein, B. (1983) *Nature (London)* **301**, 89–92.
10. de Bustros, A., Nelkin, B. D., Silverman, A., Ehrlich, G., Poiesz, B. & Baylin, S. B. (1988) *Proc. Natl. Acad. Sci. USA* **85**, 5693–5697.
11. Nelkin, B. D., Przepiorka, D., Burke, P. J., Thomas, E. D. & Baylin, S. B. (1991) *Blood* **77**, 2431–2434.
12. Baylin, S. B., Makos, M., Wu, J. J., Yen, R. W., de Bustros, A., Vertino, P. & Nelkin B. D. (1991) *Cancer Cells* **3**, 383–390.
13. Merlo, A., Herman, J. G., Mao, L., Lee, D. J., Gabrielson, E., Burger, P., Baylin, S. B. & Sidransky, D. (1995) *Nat. Med.* **1**, 686–692.
14. Ohtani-Fujita, N., Fujita, T., Aoike, A., Osifchin, N. E., Robbins, P. D. & Sakai, T. (1993) *Oncogene* **8**, 1063–1067.
15. Herman, J. G., Latif, F., Weng, Y., Lerman, M. I., Zbar, B., Liu, S., Samid, D., Duan, D. S., Gnarra, J. R., Linehan, W. M. & Baylin, S. M. (1994) *Proc. Natl. Acad. Sci. USA* **91**, 9700–9704.
16. Royer-Pokora, B. & Schneider, S. (1992) *Genes Chromosomes Cancer* **5**, 132–140.
17. Makos-Wales, M., Biel, M. A., El Deiry, W., Nelkin, B. D., Issa, J-P., Cavenee, W. K., Kuerbitz, S. J. & Baylin, S. B. (1995) *Nat. Med.* **1**, 570–577.
18. Szyf, M. (1994) *Trends Pharmacol. Sci.* **15**, 233–238.
19. Szyf, M. (1996) *Pharmacol. Ther.* **70**, 1–37.
20. Szyf, M., Avraham-Haetzni, K., Reifman, A., Shlomai, J., Kaplan, F., Oppenheim, A. & Razin A. (1984) *Proc. Natl. Acad. Sci. USA* **81**, 3278–3282.
21. Kautiainen, T. L. & Jones, P. A. (1986) *J. Biol. Chem.* **261**, 1594–1598.
22. el-Deiry, W. S., Nelkin, B. D., Celano, P., Yen, R. W., Falco, J. P., Hamilton, S. R. & Baylin, S. B. (1991) *Proc. Natl. Acad. Sci. USA* **88**, 3470–3474.
23. Belinsky, S. A., Nikula, K. J., Baylin, S. B. & Issa, J. P. J. (1996) *Proc. Natl. Acad. Sci. USA* **93**, 4045–4050.
24. Wu, J., Issa, J. P., Herman, J., Bassett, D. E., Jr., Nelkin, B. D. & Baylin, S. B. (1993) *Proc. Natl. Acad. Sci. USA* **90**, 8891–8895.
25. MacLeod, A. R. & Szyf, M. (1995) *J. Biol. Chem.* **270**, 8037–8043.
26. Rouleau, J., Tanigawa, G. & Szyf, M. (1992) *J. Biol. Chem.* **267**, 7368–7377.
27. Rouleau, J., MacLeod, A. R. & Szyf, M. (1995) *J. Biol. Chem.* **270**, 1595–1601.
28. MacLeod, A. R., Rouleau, J. & Szyf, M. (1995) *J. Biol. Chem.* **270**, 11327–11337.
29. Szyf, M., Theberge, J. & Bozovic, V. (1995) *J. Biol. Chem.* **270**, 12690–12696.
30. Jones, P. A. (1985) *Cell* **40**, 485–486.
31. Tamame, M., Antequera, F., Villanueva, J. R. & Santos T. (1983) *Mol. Cell. Biol.* **3**, 2287–2297.
32. Juttermann, R., Li, E. & Jaenisch, R. (1994) *Proc. Natl. Acad. Sci. USA* **91**, 11797–11801.
33. Dean, N. M. & McKay, R. (1994) *Proc. Natl. Acad. Sci. USA* **91**, 11762–11766.
34. Yasumura, Y., Buonsassisi, V. & Sato, G. (1966) *Cancer Res.* **26**, 529–535.
35. Schwab, M., Alitalo, K., Varmus, H. E. & Bishop, M. (1983) *Nature (London)* **303**, 497–501.
36. Szyf, M., Kaplan, F., Mann, V., Gilloh, H., Kedar, E. & Razin, A. (1985) *J. Biol. Chem.* **260**, 8653–8656.
37. Szyf, M., Bozovic, V. & Tanigawa, G. (1991) *J. Biol. Chem.* **266**, 10027–10030.
38. Ausubel, F. M., Kingston, R., Moore, D., Seidman, J., Smith, J. & Struhl, K., eds. (1988) *Current Protocols in Molecular Biology (Wiley, New York)*.
39. Freedman, V. H. & Shin, S. (1974) *Cell* **3**, 355–359.
40. Mayer, R. J. & Walker, J. H. (1987) *Immunochemical Methods in Cell and Molecular Biology* (Academic, London).
41. Szyf, M., Milstone, D. S., Schimmer, B. P., Parker, K. L. & Seidman, J. G. (1990) *Mol. Endocrinol.* **4**, 1144–1152.
42. Plumb, J. A., Wishart, C., Setanoians, A., Morrison, J. G., Hamilton, T., Bicknell, S. R. & Kaye, S. B. (1994) *Biochem. Pharmacol.* **47**, 257–266.
43. Szyf, M., Rouleau, J., Theberge, J. & Bozovic, V. (1992) *J. Biol. Chem.* **267**, 12831–12836.
44. Bestor, T. H., Laudano, A., Mattaliano, R. & Ingram, V. (1988) *J. Mol. Biol.* **203**, 971–983.
45. Walder, R. Y. & Walder, J. A. (1988) *Proc. Natl. Acad. Sci. USA* **85**, 5011–5015.
46. Szyf, M., Schimmer, B. P. & Seidman, J. G. (1989) *Proc. Natl. Acad. Sci. USA* **86**, 6853–6857.
47. Keshet, E. & Cedar, H. (1983) *Nucleic Acids Res.* **11**, 3571–3580.
48. Szyf, M., Tanigawa, G. & McCarthy, P. L., Jr. (1990) *Mol. Cell. Biol.* **10**, 4396–4340.
49. Jones, P. A., Wolkowicz, M. J., Rideout, W. M., III, Gonzales, F. A., Marziasz, C. M., Coetzee, G. A. & Tapscott, S. J. (1990) *Proc. Natl. Acad. Sci. USA* **87**, 6117–6121.
50. Issa, J. P., Zehnbauer, B. A., Civin, C. I., Collector, M. I., Sharkis, S. J., Davidson, N. E., Kaufmann, S. H. & Baylin, S. B. (1996) *Cancer Res.* **56**, 973–977.
51. Herman, J. G., Jen, J., Merlo, A., & Baylin, S. B. (1996) *Cancer Res.* **56**, 722–727.
52. Zahler, A. M., Williamson, J. R., Cech, T. R. & Prescott, D.M. (1991) *Nature (London)* **350**, 718–720.
53. Krieg, A. M., Yi, A. K., Matson, S., Waldschmidt, T. J., Bishop, G. A., Teasdale, R., Koretzky, G. A. & Klinman, D. M. (1995) *Nature (London)* **374**, 546–549.
54. Rideout, W. M., III, Coetzee, G. A., Olumi, A. F. & Jones, P. A. (1990) *Science* **249**, 1288–1290.
55. Laird, P. W., Jacksongrusby, L., Fazeli, A., Dickinson, S. L., Jung, W. E., Li, E., Weinberg, R. A. & Jaenisch, R. (1995) *Cell* **81**, 197–205.

UNITED STATES PATENT AND TRADEMARK OFFICE

CERTIFICATE OF CORRECTION

PATENT NO. : 5,958,771

DATED : September 28, 1999

INVENTOR(S) : Bennett et al.

It is certified that error appears in the above-identified patent and that said Letters Patent is hereby corrected as shown below:

At Col 17, Line 9, please delete "to liposome" and insert therefor –to use a liposome–
At. Col. 43, Line 53, please delete "Are" and insert therefor –are–

Signed and Sealed this

Twelfth Day of December, 2000

Attest:

Attesting Officer

Q. TODD DICKINSON

Director of Patents and Trademarks